

Panel Experiments and Dynamic Causal Effects: A Finite Population Perspective*

Iavor Bojinov [†] Ashesh Rambachan [‡] Neil Shephard [§]

November 15, 2021

Abstract

In panel experiments, we randomly expose multiple units to different treatments and measure their subsequent outcomes, sequentially repeating the procedure numerous times. Using the potential outcomes framework, we define finite population dynamic causal effects that capture the relative effectiveness of alternative treatment paths. For the leading example, known as the lag- p dynamic causal effects, we provide a nonparametric estimator that is unbiased over the randomization distribution. We then derive the finite population limiting distribution of our estimators as either the sample size or the duration of the experiment increases. Our approach provides a new technique for deriving finite population central limit theorems that exploits the underlying Martingale property of unbiased estimators. We further describe two methods for conducting inference on dynamic causal effects: a conservative test for weak null hypotheses of zero average causal effects using the limiting distribution and an exact randomization-based test for sharp null hypotheses. We also derive the finite population limiting distribution of commonly-used linear fixed effects estimators, showing that these estimators perform poorly in the presence of dynamic causal effects. We conclude with a simulation study and an empirical application where we reanalyze a lab experiment on cooperation.

Keywords: Panel data, dynamic causal effects, potential outcomes, finite population, nonparametric.

*We thank Gary Chamberlain for early conversations about this project. We especially thank James Andreoni and Larry Samuelson for kindly sharing their data. All remaining errors are our own. Rambachan gratefully acknowledge financial support from the NSF Graduate Research Fellowship under Grant DGE1745303.

[†]Technology and Operations Management Unit, Harvard Business School: ibojinov@hbs.edu

[‡]Department of Economics, Harvard University: asheshr@g.harvard.edu

[§]Department of Economics and Department of Statistics, Harvard University: shephard@fas.harvard.edu

1 Introduction

Panel experiments, where we sequentially expose units to a random treatment, measure their response and repeat the procedure for a fixed period of time, form the basis of causal inference in many areas of biostatistics (e.g., [Murphy et al. \(2001\)](#)), epidemiology (e.g., [Robins \(1986\)](#)), and psychology (e.g., [Lillie et al. \(2011\)](#)). In experimental economics, many authors recognize the benefits of panel-based experiments, for instance [Bellemare et al. \(2014, 2016\)](#) highlighted the potentially large gains in power and [Czibor et al. \(2019\)](#) emphasized that panel-based experiments may help uncover heterogeneity across units. Despite these benefits, however, panel experiments are used infrequently in part due to the lack of a formal statistical framework and concerns about how the impact of past treatments on subsequent outcomes may induce biases in conventional estimators ([Charness et al., 2012](#)). In practice, most authors typically assume away this complication by requiring that the outcomes only depend on contemporaneous treatment, what is often called the “no carryover assumption” (e.g., [Abadie et al. \(2017\)](#), [Athey and Imbens \(2018\)](#), [Athey et al. \(2018\)](#), [Imai and Kim \(2019b\)](#), [Imai and Kim \(2019a\)](#), [de Chaisemartin and D'Haultfoeuille \(2019\)](#), [Arkhangelsky and Imbens \(2019\)](#)). Even when researchers allow for such carryover effects, they almost solely focus on incorporating the uncertainty due to sampling units from some large (potentially infinite) super-population as opposed to the design-based uncertainty, which arises due to the random exposure of the treatment ([Abadie et al., 2020](#)).

In this paper, we tackle these challenges by defining a variety of new panel-based dynamic causal estimands without evoking super-population assumptions nor restrictions on the extent to which treatments can impact subsequent outcomes. Our approach builds on the potential outcomes formulation of causal inference ([Neyman, 1923](#); [Kempthorne, 1955](#); [Cox, 1958](#); [Rubin, 1974](#)) and takes a purely design-based perspective on uncertainty, allowing us to be agnostic to the outcomes model and avoid assumptions about hypothetical super-populations. Our main estimands are various averages of lag- p dynamic causal effects, which capture how a change in treatment affects outcomes after p periods.¹ For these estimators, we provide nonparametric estimators that are unbiased over the randomization

¹Our dynamic causal effects also provide a useful perspective to the vast literature on observational panel data in econometrics (e.g., the reviews of [Arellano \(2003\)](#), [Arellano and Bonhomme \(2012\)](#)) that tend to avoid formal discussions of causal effects in the modern sense that explicitly appeals to potential outcome functions to define counterfactuals (e.g., [Imbens and Rubin \(2015\)](#), [Hernan and Robins \(2019\)](#)) or directed acyclic graphs to define causal structures (e.g., [Pearl and Mackenzie \(2018\)](#)).

distribution. Then, by exploiting the underlying Martingale property of our unbiased estimators, we derive their finite population asymptotic distribution as either the number of sample periods, experimental units, or both increases. This is a new technique for proving finite population central limit theorems, which may be broadly useful and of independent interest to researchers.

Next, we describe two methods for conducting inference on dynamic causal effects. The first uses the limiting distribution to perform conservative, nonparametric inference on the weak null hypothesis of no average dynamic causal effect. The second provides an exact, randomization test for the sharp null of no treatment effect at any point in time. We then highlight the broader usefulness of our framework by deriving the finite population probability limit of a variety of standard linear estimation strategies commonly employed on panel data, such as the unit fixed effects estimator and the two-way fixed effects estimator. Our results show that such linear estimators are biased for the dynamic causal effects because of the presence of carryover effects and possible serial correlation in the treatment assignment mechanism.

Finally, we illustrate our theoretical results in an extensive simulation study and by applying our framework to reanalyze a panel-based experiment. The simulation begins by showing the validity of our finite population central limit theorems under a variety of assumptions about the underlying potential outcomes and treatment assignment mechanism. We then confirm that conservative tests based on the asymptotic approximation to the randomization distribution of our nonparametric estimator control size well in finite populations and have good rejection rates against a variety of alternatives. We finish by re-analyzing an experiment conducted in [Andreoni and Samuelson \(2006\)](#), which studies cooperative behavior in game theory. The experiment has a natural panel structure—each participant played a twice-repeated prisoners’ dilemma many times, and the payoff structure of the game was randomly varied across each play. We confirm the authors’ original hypothesis that the payoff structure of the twice repeated prisoners’ dilemma has significant effects on cooperative behavior. Moreover, we provide new, suggestive evidence of dynamic causal effects in this experiment—the payoff structure of previously played games may affect cooperative behavior in the current game.

Our framework builds up and generalizes the notation and concepts introduced for analyzing time series experiments in [Bojinov and Shephard \(2019\)](#) in three crucial ways.² First, we focus on a much

²See also [Rambachan and Shephard \(2019\)](#) for a discussion on how to connect [Bojinov and Shephard \(2019\)](#) to influential works in macroeconomics and financial econometrics.

richer class of causal estimands, which answer a broader set of causal questions. Second, we derive two new finite population central limit theorems as the size of the population grows, and as both the duration and population size increase. Third, we compute the bias present in standard linear estimators in the presence of dynamic causal effects and serial correlation in the treatment assignment probabilities. Throughout our exposition, we will explain how to derive the results developed in [Bojinov and Shephard \(2019\)](#) as a special case of our more general formulation.

Our framework is importantly distinct from earlier work by [Robins \(1986\)](#) and co-authors, that uses treatment paths for causal panel data analysis because the solely focus on providing super-population (or sampling-based) inference methods. In contrast, we avoid super-population arguments entirely and make our inference completely conditional on the potential outcomes.³ This design-based perspective provides the first generalization of the finite population literature in cross-sectional causal inference, as reviewed in [Imbens and Rubin \(2015\)](#), to panel experiments.

Overview of the paper: In Section 2, we define potential outcome panels, for which we formally define a series of dynamic causal estimands of interest. In Section 3, we provide a nonparametric estimator for our dynamic causal estimands, derive their finite sample properties, and provide finite population central limit theorems that we use for inference. In Section 4, we obtain the finite population limiting distributions of standard linear estimation methods for potential outcome panels, such as the unit fixed effects estimator and the two-way fixed effects estimator. In Section 5, we detail a simulation study, and in Section 6, we use our framework to reanalyze a panel experiment conducted by Andreoni. The appendix collects all technical proofs as well as additional simulations and empirical results.

Notation: For an integer $t \geq 1$ and a variable A_t , we write $A_{1:t} := (A_1, \dots, A_t)$. We compactly write index sets as $[N] := \{1, \dots, N\}$ and $[T] := \{1, \dots, T\}$. Finally, for a random variable $W_{i,t}$ observed over $i \in [N]$ and $t \in [T]$, define its average over t as $\bar{W}_i := \frac{1}{T} \sum_{t=1}^T W_{i,t}$, its average over i as

³Avoiding super-populations in the definition of dynamic causal estimands are often attractive in panel data applications. For example, a company only operates in a finite number of markets (e.g., states or cities within the United States) and can conduct advertising or promotional experiments across these markets. Assuming that we can sample additional markets to make superpopulation arguments may be difficult to justify scientifically, despite its elegance as a modelling device. However, in other cases, super-population arguments may be entirely natural, given the scientific question at hand. For example, in the mental healthcare digital experiments of [Boruvka et al. \(2018\)](#), it is compelling to use sampling-based arguments as the experimental units are drawn from a larger group of patients for whom we wish to make inference on as, if successful, the technology will be broadly rolled out.

$\bar{W}_t := \frac{1}{N} \sum_{i=1}^N W_{i,t}$ and its average over both i and t as $\bar{X} := \frac{1}{NT} \sum_{t=1}^T \sum_{i=1}^N W_{i,t}$.

2 Potential outcome panel and dynamic causal effects

2.1 Treatment panels and potential outcomes

Consider a panel in which N units (e.g., individuals, firms, or countries) indexed by $i \in [N]$ are observed over $t \in [T]$ time periods. For each unit i and period t , we administer a treatment $W_{i,t} \in \mathcal{W}$. Throughout this paper, we assume that the treatment is a random variable. Whenever the treatment is binary, that is $\mathcal{W} = \{0, 1\}$, we follow convention and refer to “1” as treatment and “0” as control.

The *treatment path* for unit i is the sequence of treatments that is administered to unit i over the entire sample period, denoted $W_{i,1:T} = (W_{i,1}, \dots, W_{i,T})' \in \mathcal{W}^T$. The *time- t cross-sectional treatment assignment* describes the treatments received by all units at period t , denoted $W_{1:N,t} = (W_{1,t}, \dots, W_{N,t})' \in \mathcal{W}^N$. Finally, the *treatment panel* is the $N \times T$ matrix $W_{1:N,1:T} \in \mathcal{W}^{N \times T}$ that summarizes the treatments assigned to all units over the entire sample period, where

$$W_{1:N,1:T} = \begin{pmatrix} W_{1:N,1}, \dots, W_{1:N,T} \end{pmatrix} = \begin{pmatrix} W'_{1,1:T} \\ \vdots \\ W'_{N,1:T} \end{pmatrix}.$$

Each column of $W_{1:N,1:T}$ is the cross-sectional treatment assignment for a particular period and each row is the treatment path for a particular unit over the sample period.

We next define a *potential outcome*, which describes what would be observed for a particular unit at a fixed point in time along a given treatment panel.

Definition 1. *The potential outcome for unit- i at time- t along treatment panel $w_{1:N,1:T} \in \mathcal{W}^{N \times T}$ is written as $Y_{i,t}(w_{1:N,1:T})$.*

In principle, the potential outcome can depend upon the entire treatment panel allowing for arbitrary spillovers across units and time periods. The idea of focusing paths and defining potential outcomes as a function of treatment paths first appears in [Robins \(1986\)](#) and has been further developed in subsequent work such as [Robins \(1994\)](#), [Murphy et al. \(2001\)](#) and [Boruvka et al. \(2018\)](#).⁴ Our work

⁴[Hernan and Robins \(2019\)](#) provide a modern, textbook treatment of this literature.

differs from this approach by avoiding super-population arguments entirely. All our estimands and inference procedures are conditioned on the potential outcomes and all uncertainty arises solely from the random assignment of treatment paths. Our work is therefore the natural extension of the potential outcomes cross-sectional causal inference framework to the panel setting.

[Abadie et al. \(2017\)](#) highlight the appeal of this finite-sample, design-based perspective in panel data applications in econometrics. However, the panel-based potential outcome model developed in that work contains no dynamics as the authors primarily focus on cross-sectional data with an underlying cluster structure.⁵ Our finite-sample perspective and emphasis on the causal effects of treatment paths are important contrasts to much of the existing literature on panel data analysis in econometrics. For example, [Arellano and Bonhomme \(2012\)](#) reviews non-linear panel data methods, which typically focus on estimating non-linear *contemporaneous* causal effects.⁶ Recently, [Hull \(2018\)](#) and [Han \(2019\)](#) consider a potential outcome model similar to ours but rely on super-population arguments, similar to [Robins \(1986\)](#), to perform inference.

2.2 The potential outcome panel model

We now define the potential outcomes panel model by developing four assumptions that we maintain through the remainder of the paper. The first is a generalization of the non-anticipating treatment assumption studied in the time series setting by [Bojinov and Shephard \(2019\)](#). This assumption restricts the potential outcomes for a unit in a given period not to be affected by future treatments while allowing them to depend on the entire treatment path up to that period.

Assumption 1. *The potential outcomes are **non-anticipating** if, for all $i \in [N]$ and $t \in [T]$, and $w_{1:N,1:T}, \tilde{w}_{1:N,1:T} \in \mathcal{W}^{N \times T}$*

$$Y_{i,t}(w_{1:N,1:T}) = Y_{i,t}(\tilde{w}_{1:N,1:T}),$$

whenever $w_{1:N,1:t} = \tilde{w}_{1:N,1:t}$.

Non-anticipation still allows an arbitrary dependence on past and contemporaneous treatments as well as the treatments of other units. We now introduce an assumption that restricts treatment

⁵Similarly, [Athey and Imbens \(2018\)](#), [Athey et al. \(2018\)](#) and [Arkhangelsky and Imbens \(2019\)](#) also introduce a potential outcome model for panel data, but assume away carryover effects.

⁶For example, [Arellano et al. \(2017\)](#) apply state-of-the-art non-linear panel data methods to estimate the contemporaneous causal effect of earnings fluctuations on household consumption.

spillovers across units, meaning that the potential outcomes for a unit are only impacted by their own treatment paths. This idea was first introduced by Cox (1958). Combining this assumption with a further requirement that every unit receives the same version of the treatment is often referred to as the “Stable Unit Treatment Value Assumption,” in cross-sectional applications (Rubin, 1980) or the “Temporal Stable Unit Treatment Value Assumption” in time series experiments (Bojinov and Shephard, 2019).

Assumption 2. *The potential outcomes satisfy the **Temporal Stable Unit Treatment Value Assumption** (TSUTVA) if, for all $i \in [N]$ and $t \in [T]$, and $w_{1:N,1:T}, \tilde{w}_{1:N,1:T} \in \mathcal{W}^{N \times T}$*

$$Y_{i,t}(w_{1:N,1:T}) = Y_{i,t}(\tilde{w}_{1:N,1:T}),$$

whenever $w_{i,1:T} = \tilde{w}_{i,1:T}$.

Under Assumption 1 and Assumption 2, the potential outcome for unit i at time t only depends on the treatment path for unit i up to time t . Throughout the paper, we maintain both Assumption 1 and Assumption 2, allowing us to simplify the notation for the potential outcomes for unit i at time t to be $Y_{i,t}(w_{i,1:t})$. Denote the collection of potential outcomes for unit i at time t for all possible panel treatment paths as $Y_{i,t}(\bullet) = \{Y_{i,t}(w_{i,1:t}) : w_{i,1:t} \in \mathcal{W}^t\}$. Similarly, $Y_{1:N,1:T}(\bullet) = \{Y_{i,t}(\bullet) : i \in [N], t \in [T]\}$ denotes the collection of potential outcomes for all units across all time periods.

We further require that the treatment assignment mechanism at time t only depends on past treatment assignments and observed outcomes, meaning that the treatment assignment in a given period may not depend on future nor unobserved past potential outcomes. We refer to this assumption as *non-anticipating treatments*, following the time series work of Bojinov and Shephard (2019).

Assumption 3. *The treatments are **non-anticipating** if, for each $t \in [T]$, for all $w_{1:N,1:t-1} \in \mathcal{W}^{N \times (t-1)}$*

$$\Pr(W_{1:N,t} | W_{1:N,1:t-1} = w_{1:N,1:t-1}, Y_{1:N,1:T}(\bullet)) = \Pr(W_{1:N,t} | W_{1:N,1:t-1} = w_{1:N,1:t-1}, Y_{1:N,1:t-1}(w_{1:N,1:t-1})).$$

We think of this as the panel data analogue of an unconfounded or ignorable treatment assignment mechanism in the literature on cross-sectional causal inference (reviewed in Imbens and Rubin (2015)).

Under Assumption 3, the treatment assignment at any point in time may depend on the entire treatment panel up to the previous period as well as all prior, observed outcomes. This allows for a rich set of possible treatment assignment mechanisms.

To connect the observed outcomes with the potential outcomes, we assume that every unit takes the treatment that was offered, removing the possibility of subject non-compliance.⁷

Assumption 4. *For an observed treatment path $w_{1:N,1:T}^{obs}$, the observed outcome is given by $y_{1:N,1:T}^{obs} = Y_{1:N,1:T}(w_{1:N,1:T}^{obs})$.*

Definition 2. *A panel of outcomes and treatments which obey Assumptions 1-4 is a **potential outcome panel**.*

For the case where $N = 1$, the potential outcome panel reduces to the definition of a potential outcome time series in [Bojinov and Shephard \(2019\)](#). For $T = 1$, the potential outcome panel reduces to the canonical Neyman-Rubin causal model ([Holland, 1986](#); [Imbens and Rubin, 2015](#)).

2.2.1 The linear potential outcome panel

Much of the dynamic panel data literature focuses on linear models, which can be expressed as a special case of our general setup.

Definition 3. *A linear potential outcome panel is a potential outcome panel, in which the potential outcomes additionally satisfy*

$$Y_{i,t}(w_{i,1:t}) = \beta_{i,t,0}w_{i,t} + \dots + \beta_{i,t,t-1}w_{i,1} + \epsilon_{i,t} \quad \forall t \geq 1,$$

where the coefficients $\beta_{i,t,0:t-1}$ and the residual $\epsilon_{i,t}$ do not depend upon treatments.

This model assumes that the potential outcome for unit i at time t is simply a linear function of unit i 's treatment path plus a residual $\epsilon_{i,t}$ term that does not vary with the treatments. Otherwise, the residual is completely unconstrained.

In some cases, we may wish to place further restrictions on the coefficients in a linear potential outcome panel. We formalize these restrictions with the following definition.

⁷In some applications, this assumption may be unrealistic. For example, in a panel-based clinical trial, we may worry that patients do not properly adhere to the treatments that are assigned.

Definition 4. For a linear potential outcome panel, the coefficients $\beta_{i,t,s}$ are **dynamic causal coefficients**. Moreover, the dynamic causal coefficients are

- **time-invariant** if $\beta_{i,t,s} = \beta_{i,s}$, for all $t \in [T]$, and $s = 0, \dots, t-1$.
- **homogenous** if $\beta_{i,t,s} = \beta_{t,s}$, for all $i \in [N]$ and $s = 0, \dots, t-1$.

If $\beta_{i,t,s} = \beta_s$ for all $i \in [N]$, $t \in [T]$, $s = 0, \dots, t-1$ then the dynamic causal coefficients are homogeneous and time-invariant.

A leading example of a linear potential outcome panel is the autoregressive potential outcome panel.

Example 1. An autoregressive potential outcome panel is a potential outcome panel, in which the potential outcomes obey

$$Y_{i,t}(w_{i,1:t}) = \phi_{i,t,0}Y_{i,t-1}(w_{i,1:t-1}) + \dots + \phi_{i,t,t-2}Y_{i,1}(w_{i,1}) + \beta_{i,t,0}w_{i,t} + \dots + \beta_{i,t,t-1}w_{i,1} + \epsilon_{i,t} \quad \forall t > 1,$$

$$Y_{i,1}(w_{i,1}) = \beta_{i,1,0}w_{i,1} + \epsilon_{i,1},$$

where the coefficients $\phi_{i,t,0:t-2}$, $\beta_{i,t,0:t-1}$ and the residuals $\epsilon_{i,1:t}$ do not depend on treatments. It is a simple exercise to solve out the potential outcomes to produce the linear potential outcome given in Definition 3.

Example 1 allows for heterogeneity in the parameters across units as well as arbitrary dependence across units and time through $\epsilon_{i,t}$. It is therefore a vast generalization of the non-causal autoregressive econometric panel model associated with, for example, Nerlove (1971), Nickell (1981), Anderson and Hsiao (1982), Arellano and Bond (1991) and the review of Arellano (2003).⁸ The linear potential outcome panel is the panel extension of the potential autoregression time series introduced by Bojinov and Shephard (2019).

⁸Allowing for heterogeneity in panel data models is useful in many empirical applications. For example, in many economic settings, there is extensive heterogeneity across units such as in modeling income processes (Browning et al., 2010) and estimating the dynamic response of consumption to earnings (Arellano et al., 2017). Time-varying heterogeneity is also an important feature. For example, it is a classic point of emphasis in studying human capital formation and education investments – see Ben-Porath (1967), Griliches (1977) and more recently, Cunha et al. (2006) and Cunha et al. (2010).

2.2.2 Special case of the non-interference assumption

Depending on the design of the panel-based experiment, there are two important special cases of non-anticipating treatments (Assumption 3), which impose additional forms of conditional independence across treatments. Let $W_{-i,t} := (W_{1,t}, \dots, W_{i-1,t}, W_{i+1,t}, \dots, W_{N,t})$ and $\mathcal{F}_{1:N,t,T}$ be the filtration generated by $W_{1:N,1:t}$ and $Y_{1:N,1:T}(\bullet)$.

Assumption 5. *Maintain Assumption 3. Then, the treatments are*

1. *contemporaneously non-interfering for unit- i if*

$$\Pr(W_{i,t}|W_{-i,t}, \mathcal{F}_{1:N,t-1,T}) = \Pr(W_{i,t}|W_{1:N,1:t-1} = w_{1:N,1:t-1}, Y_{1:N,1:t-1}(w_{1:N,1:t-1}))$$

for all $t \in [T]$.

2. *non-interfering for unit- i if*

$$\Pr(W_{i,t}|W_{-i,t}, \mathcal{F}_{1:N,t-1,T}) = \Pr(W_{i,t}|W_{i,1:t-1} = w_{i,1:t-1}, Y_{i,1:t-1}(w_{i,1:t-1}))$$

for all $t \in [T]$.

Contemporaneous non-interference imposes that, conditional on all past treatments and outcomes, the time- t treatments are selected independently across units. Meaning that information from past observed outcomes and treatments across all units may determine the treatment probabilities at time t . For example, if we notice that, on average, treatment $w \in \mathcal{W}$ is outperforming all other treatments, we may increase the probability of administering treatment w to all subjects at time t . Non-interference further imposes that conditional on its own past treatments and outcomes, the treatment for unit i at time t is independent of the past treatments and outcomes of all other units. For example, the Bernoulli randomization mechanism, where $\Pr(W_{i,t}|W_{-i,t}, \mathcal{F}_{1:N,t-1,T}) = \Pr(W_{i,t})$ for all $i \in [N]$ and $t \in [T]$, is non-interfering. The following example provides less trivial randomization mechanisms to illustrate these assumptions.

Example 2. *Suppose $W_{i,t} \in \{0, 1\}$ and $\lambda \in (0, 1)$. The following two treatment assignments are contemporaneously non-interfering for unit i :*

1. *Dependence on past binary treatments:* $\Pr(W_{i,t} = 1 | W_{-i,t} = w_{-i,t}, \mathcal{F}_{1:N,t-1,T}) = \lambda + (1 - \lambda)\bar{w}_{t-1}^{obs}$.
2. *Dependence on past binary outcomes:* $\Pr(W_{i,t} = 1 | W_{-i,t} = w_{-i,t}, \mathcal{F}_{1:N,t-1,T}) = \lambda + (1 - \lambda)\bar{y}_{t-1}^{obs}$.

The following two treatment assignments are non-interfering for unit i :

1. *Dependence on past binary treatments:* $\Pr(W_{i,t} = 1 | W_{-i,t} = w_{-i,t}, \mathcal{F}_{1:N,t-1,T}) = \lambda + (1 - \lambda)w_{i,t-1}^{obs}$.
2. *Dependence on past binary outcomes:* $\Pr(W_{i,t} = 1 | W_{-i,t} = w_{-i,t}, \mathcal{F}_{1:N,t-1,T}) = \lambda + (1 - \lambda)y_{i,t-1}^{obs}$.

2.3 Dynamic causal effects

The purpose of developing the treatment paths and potential outcomes was to build the necessary notation and concepts for defining causal effects that capture the relative effectiveness of alternative treatment paths on the outcome of interest.

For a potential outcome panel, a *dynamic causal effect* compares the potential outcomes for unit- i at time- t along different treatment paths, denoted by

$$\tau_{i,t}(w_{i,1:t}, \tilde{w}_{i,1:t}) := Y_{i,t}(w_{i,1:t}) - Y_{i,t}(\tilde{w}_{i,1:t}), \quad (1)$$

for $w_{i,1:t}, \tilde{w}_{i,1:t} \in \mathcal{W}^t$. The term “dynamic” is used to emphasize that the potential outcomes are functions of the full treatment path and that the effects vary across both units and time.

Since we are taking a design-based perspective, we regard all the potential outcomes $Y_{i,t}(\bullet)$ as fixed but unknown, or equivalently we condition on the set of all potential outcomes throughout our exposition. The challenge in estimating dynamic causal effects is then our inability to observe all relevant outcomes.

Similar to the Neyman-Rubin causal model, we are more interested in averages of these dynamic causal effects. For example, we could average over units at a fixed time period t to get the average dynamic causal effect at time t , or we could average over time periods for a fixed unit i to get the average dynamic causal effect for unit i . We could also average over both units and time periods. In the rest of this section, we use these unit- i time- t dynamic causal effects to build up causal estimands of interest.

2.3.1 Lag- p dynamic causal effects and average treatment effects

Since the number of potential outcomes grows exponentially with the time period t , there is a considerable number of possible dynamic causal effects. To make progress, we restrict our attention to a core class:

Definition 5. *Let $\mathbf{w}, \tilde{\mathbf{w}} \in \mathcal{W}^{p+1}$. The i, t -th lag- p dynamic causal effect is*

$$\tau_{i,t}(\mathbf{w}, \tilde{\mathbf{w}}; p) := \tau_{i,t}(\{w_{i,1:t-p-1}^{obs}, \mathbf{w}\}, \{w_{i,1:t-p-1}^{obs}, \tilde{\mathbf{w}}\}).$$

The i, t -th lag- p dynamic causal effect measures the difference between the outcomes from following treatment path \mathbf{w} from period $t - p$ to t compared to the alternative path $\tilde{\mathbf{w}}$, fixing the treatments for unit i to follow the observed path up to time $t - p - 1$.⁹ We use the bold notation for the treatments that define the dynamic causal effects to help differentiate them from all other possible treatment paths. We also intentionally drop the subscripts because later we will average the dynamic causal effects across both time and units for a particular \mathbf{w} and $\tilde{\mathbf{w}}$.

Example 3 (Causal effects for linear potential outcome panel models). *In the case of a linear potential outcome panel (Definition 3), i, t -th lag- p dynamic causal effects are linear functions of the difference between the treatment and counter-factual paths:*

$$\tau_{i,t}(\mathbf{w}, \tilde{\mathbf{w}}; p) = \sum_{s=0}^p \beta_{i,t,s} (w_{t-s} - \tilde{w}_{t-s}),$$

where both $\mathbf{w}, \tilde{\mathbf{w}} \in \mathcal{W}^{p+1}$.

We use the i, t -th lag- p dynamic causal effects as building blocks of many other interesting causal estimands. In particular, by restricting the paths \mathbf{w} and $\tilde{\mathbf{w}}$ to share some common features, we obtain the weighted average i, t -th lag- p dynamic causal effect.

Definition 6. *The weighted average i, t -th lag- p, q dynamic causal effect is defined as*

$$\tau_{i,t}^\dagger(\mathbf{w}, \tilde{\mathbf{w}}; p, q) := \sum_{\mathbf{v} \in \mathcal{W}^{p-q+1}} a_{\mathbf{v}} \left\{ Y_{i,t}(w_{i,1:t-p-1}^{obs}, \mathbf{w}, \mathbf{v}) - Y_{i,t}(w_{i,1:t-p-1}^{obs}, \tilde{\mathbf{w}}, \mathbf{v}) \right\},$$

⁹Defining dynamic causal effects conditional on the observed past treatments $w_{i,1:t-p-1}^{obs}$ is in line with the common focus on the average treatment effect on the treatment (e.g. [Lechner \(2011\)](#) and [Imbens and Rubin \(2015\)](#)). See [Bojinov and Shephard \(2019\)](#) for a more in-depth discussion as well as a strategy known as “stepping” to reduce the dependence on the observed treatment path.

where $\mathbf{w}, \tilde{\mathbf{w}} \in \mathcal{W}^q$, for integers p, q satisfying $q > 0$, $p \geq 0$ and $p + 1 \leq q$, while $\{a_{\mathbf{v}}\}$ are non-stochastic weights that satisfy $\sum_{\mathbf{v} \in W^p} a_{\mathbf{v}} = 1$ and $a_{\mathbf{v}} \geq 0$ for all $\mathbf{v} \in \mathcal{W}^{p-q+1}$.

The weighted average i, t -th lag- p, q dynamic causal effect summarizes the effect of switching the treatment path between period $t - p$ and period $t - p + q$ from \mathbf{w} to $\tilde{\mathbf{w}}$ on outcomes at time t by averaging across all possible treatment paths from period $t - p + q + 1$ to period t . The weights $a_{\mathbf{v}}$ are context specific and may be freely selected by the researcher. Usually, we select uniform weights.

Example 4 (Causal effects for linear potential outcome panel models continued). *Continuing with the linear potential outcome panel, the weighted average i, t -th lag- p, q dynamic causal effects are also linear functions of the difference between the treatment and counter-factual paths:*

$$\tau_{i,t}^{\dagger}(\mathbf{w}, \tilde{\mathbf{w}}; p, q) = \sum_{s=0}^q \beta_{i,t,p+s} (w_{t-p+s} - \tilde{w}_{t-p+s})$$

for $\mathbf{w}, \tilde{\mathbf{w}} \in \mathcal{W}^q$,

For binary treatment, setting $N = q = 1$ gives us the special case of the weighted average i, t -th lag- p, q dynamic causal effect studied in [Bojinov and Shephard \(2019\)](#). This is the effect of switching the treatment at time $t - p$ from treatment to control on outcomes at time t by averaging across all possible treatment paths from period $t - p + 1$ to period t . Whenever $q = 1$, we drop the q from the notation, simply writing

$$\tau_{i,t}^{\dagger}(w, \tilde{w}; p) := \tau_{i,t}^{\dagger}(w, \tilde{w}; p, 1) = \sum_{\mathbf{v} \in W^{p-q+1}} a_{\mathbf{v}} \left\{ Y_{i,t}(w_{i,1:t-p-1}^{obs}, w, \mathbf{v}) - Y_{i,t}(w_{i,1:t-p-1}^{obs}, \tilde{w}, \mathbf{v}) \right\}.$$

Example 5 (Causal effects for linear potential outcome panel models continued). *Continuing with the linear potential outcome panel, for $w, \tilde{w} \in \mathcal{W}$ and $q = 1$,*

$$\tau_{i,t}^{\dagger}(\mathbf{w}, \tilde{\mathbf{w}}; p) = \beta_{i,t,p} (w - \tilde{w}).$$

The following example illustrates the i, t -th lag- p dynamic causal effect, showing that it can be used to capture many interesting causal effects.

Example 6. *Assume the treatment is binary, $\mathcal{W} = \{0, 1\}$.*

Setting $p = 0$ gives us $\tau_{i,t}(1, 0; 0) = \tau_{i,t}^\dagger(1, 0; 0) = Y_{i,t}(w_{i,1:t-1}^{obs}, 1) + Y_{i,t}(w_{i,1:t-1}^{obs}, 0)$, the unit- i time- t contemporaneous causal effect that measures the instant impact of administering treatment as opposed to control on our outcome of interest.

Now set $p = 1$. Then,

$$\tau_{i,t}((1, 0), (0, 0); 1) = Y_{i,t}(w_{i,1:t-2}^{obs}, 1, 0) - Y_{i,t}(w_{i,1:t-2}^{obs}, 0, 0),$$

measures the impact of giving a treatment as opposed to control at time $t - 1$ on the outcome, while the treatment at time t is, in both case, zero. If we instead consider the case when the treatment at time t is 1 we get,

$$\tau_{i,t}((1, 1), (0, 1); 1) = Y_{i,t}(w_{i,1:t-2}^{obs}, 1, 1) - Y_{i,t}(w_{i,1:t-2}^{obs}, 0, 1).$$

The uniform weighted average i, t lag-1 dynamic causal effect is then,

$$\begin{aligned} \tau_{i,t}^\dagger(1, 0; 1) &= \frac{1}{2} \left[\{Y_{i,t}(w_{i,1:t-2}^{obs}, 1, 0) - Y_{i,t}(w_{i,1:t-2}^{obs}, 0, 0)\} + \{Y_{i,t}(w_{i,1:t-2}^{obs}, 1, 1) - Y_{i,t}(w_{i,1:t-2}^{obs}, 0, 1)\} \right] \\ &= \frac{1}{2} [\tau_{i,t}((1, 0), (0, 0); 1) + \tau_{i,t}((1, 1), (0, 1); 1)]. \end{aligned}$$

In other words, $\tau_{i,t}^\dagger(1, 0; 1)$ measures the average impact of changing the treatment at time $t - 1$ on the outcomes in period t .

Finally, $\tau_{i,t}((1, 1), (0, 0); 1) = Y_{i,t}(w_{i,1:t-2}^{obs}, 1, 1) - Y_{i,t}(w_{i,1:t-2}^{obs}, 0, 0)$ measures the impact of giving two consecutive treatments as opposed to controls on the outcome. The extreme version of this, $\tau_{i,t}((1 \dots, 1), (0 \dots, 0); 1)$ is the commonly studied “total” causal effect estimand.

The main estimands of interest in this paper are averages of these dynamic causal effects that summarize how the treatment impacts the experimental units.

Definition 7. For a potential outcome panel, the **time- t lag- p average dynamic causal effect** is

$$\bar{\tau}_t(\mathbf{w}, \tilde{\mathbf{w}}; p) := \frac{1}{N} \sum_{i=1}^N \tau_{i,t}(\mathbf{w}, \tilde{\mathbf{w}}; p).$$

In contrast, the **unit- i lag- p average dynamic causal effect** is

$$\bar{\tau}_i(\mathbf{w}, \tilde{\mathbf{w}}; p) := \frac{1}{T-p} \sum_{t=p+1}^T \tau_{i,t}(\mathbf{w}, \tilde{\mathbf{w}}; p).$$

Finally, the **total lag- p average dynamic causal effect** is defined as

$$\bar{\tau}(\mathbf{w}, \tilde{\mathbf{w}}; p) := \frac{1}{N(T-p)} \sum_{t=p+1}^T \sum_{i=1}^N \tau_{i,t}(\mathbf{w}, \tilde{\mathbf{w}}; p).$$

Definition 7 extends to the weighted average i, t -th lag- p dynamic causal effect by defining $\bar{\tau}^\dagger(\mathbf{w}, \tilde{\mathbf{w}}; p, q)$, $\bar{\tau}_i^\dagger(\mathbf{w}, \tilde{\mathbf{w}}; p, q)$, and $\bar{\tau}_t^\dagger(\mathbf{w}, \tilde{\mathbf{w}}; p, q)$ by replacing $\bar{\tau}_{i,t}(\mathbf{w}, \tilde{\mathbf{w}}; p)$ with $\bar{\tau}_{i,t}^\dagger(\mathbf{w}, \tilde{\mathbf{w}}; p, q)$.

Example 7. Assume a linear potential outcome panel, then,

$$\begin{aligned} \tau_{i,t}(w, \tilde{w}; p) &= \beta_{i,t,p}(w - \tilde{w}), \\ \bar{\tau}_i(w, \tilde{w}; p) &= \bar{\beta}_{i,p}(w - \tilde{w}), \\ \bar{\tau}_t(w, \tilde{w}; p) &= \bar{\beta}_{t,p}(w - \tilde{w}), \\ \bar{\tau}(w, \tilde{w}; p) &= \bar{\beta}_p(w - \tilde{w}). \end{aligned}$$

By computing the dynamic lag- p causal effects at different points in time, we can understand how the effect varies over time. Generally, dynamic causal effects allow us to ask and answer a much richer class of questions than typical cross-sectional experiments or panel experiments that make the no carryover assumption.

3 Nonparametric estimation and inference

We now develop a nonparametric Horvitz and Thompson (1952) type estimator of the i, t -th lag- p dynamic causal effects. Throughout this section, we assume that the treatment assignment mechanism is non-interfering (Assumption 5), which restricts the treatment assignment probabilities of unit i to only depend on the observed treatment and outcome paths for unit i . Under the additional assumption of probabilistic treatment, defined below, we show that our proposed estimator is unbiased for the unit- i time- t lag- p dynamic causal effects and its related averages over the treatment path assignment

mechanism. Additionally, we show that as our population grows large, an appropriately scaled and centered version of our estimator for the average lag- p dynamic causal effects becomes approximately normally distributed. These limiting results are conditional on the potential outcomes, and so they are finite population central limit theorems in the spirit of Freedman (2008) and Li and Ding (2017).

3.1 Setup: extended propensity score and probabilistic treatment

To make our notation more compact, we define the *extended propensity score*, which captures the conditional probability of a given treatment path. For each i, t , and any $\mathbf{w} = (w_1, \dots, w_{p+1}) \in \mathcal{W}^{(p+1)}$, the extended propensity score is

$$p_{i,t-p}(\mathbf{w}) := \Pr(W_{i,t-p:t} = \mathbf{w} | W_{i,1:t-p-1}, Y_{i,1:t}(W_{i,1:t-p-1}, \mathbf{w})), \quad (2)$$

and can be decomposed using the prediction decomposition.

Lemma 3.1. *For a potential outcome panel and any $\mathbf{w} \in \mathcal{W}^{(p+1)}$, the extended propensity score can be factorized as*

$$\begin{aligned} p_{i,t-p}(\mathbf{w}) &= \Pr(W_{i,t-p} = w_1 | W_{i,1:t-p-1}, Y_{i,1:t-p-1}(W_{i,1:t-p-1})) \\ &\quad \times \prod_{s=1}^p \Pr(W_{i,t-p+s} = w_{s+1} | W_{i,1:t-p-1}, W_{i,t-p:t-p+s-1} = \mathbf{w}_{1:s}, Y_{i,1:t-p+s-1}(W_{i,1:t-p-1}, \mathbf{w}_{1:s})). \end{aligned}$$

Proof. Use the prediction decomposition for treatments, given all outcomes,

$$\begin{aligned} p_{i,t-p}(\mathbf{w}) &= \Pr(W_{i,t-p} = w_1 | W_{i,1:t-p-1}, Y_{i,1:t}(W_{i,1:t-p-1}, \mathbf{w})) \\ &\quad \times \prod_{s=1}^p \Pr(W_{i,t-p+s} = w_{s+1} | W_{i,1:t-p-1}, W_{i,t-p:t-p+s-1} = \mathbf{w}_{1:s}, Y_{i,1:t}(W_{i,1:t-p-1}, \mathbf{w})). \end{aligned}$$

and then simplify using non-anticipation of treatments. \square

In panel experiments, we only observe the outcomes along the observed treatment path $Y_{i,1:t}(w_{i,1:t}^{obs})$, and so it is generally not possible to use Lemma 3.1 to compute $p_{i,t-p}(\mathbf{w})$. We can, however, compute the extended propensity score along the observed treatment path, $p_{i,t-p}(w_{i,t-p:t}^{obs})$.

We next assume that the treatment assignment $p_{i,t-p}(\mathbf{w})$ is *probabilistic*. This is a crucial assumption as it provides the only source of randomness as we treat the potential outcomes as unknown but

fixed.

Assumption 6 (Probabilistic Treatment Assignment). *Consider a potential outcome panel. Assume that, for each $i \in [N]$, $t \in [T]$, $0 < c_l < p_{i,t-p}(\mathbf{w}) < c_u < 1$ for all $\mathbf{w} \in \mathcal{W}^{(p+1)}$.*

All expectations, denoted by \mathbb{E} , are computed with respect to the probabilistic treatment assignment mechanism. We write $\mathcal{F}_{i,t-p-1}$ as the filtration generated by $W_{i,1:t-p-1}$ and $\mathcal{F}_{1:N,t-p-1}$ as the filtration generated by $W_{1:N,1:t-p-1}$. Since we treat the potential outcomes as fixed (or, equivalently, we always condition on all of the potential outcomes), conditioning on $W_{i,1:t-p-1}$ is the same as conditioning on both $W_{i,1:t-p-1}$ and $Y_{i,1:t-p-1}(W_{i,1:t-p-1})$. For example, $\mathbb{E}[W_{i,t} | \mathcal{F}_{i,t-1}] = \sum_{w \in \mathcal{W}} w p_{i,t}(w)$.

Remark 3.1. *When we develop our asymptotic arguments, we assume that the bounds c_l, c_u in Assumption 6 do not vary with N or T .*

3.2 Estimation of the i, t -th lag- p dynamic causal effect

For any $\mathbf{w}, \tilde{\mathbf{w}} \in \mathcal{W}^{(p+1)}$, recall the i, t -th lag- p dynamic causal effect is $\tau_{i,t}(\mathbf{w}, \tilde{\mathbf{w}}; p) = Y_{i,t}(w_{i,1:t-p-1}^{obs}, \mathbf{w}) - Y_{i,t}(w_{i,1:t-p-1}^{obs}, \tilde{\mathbf{w}})$. Define the nonparametric estimator of $\tau_{i,t}(\mathbf{w}, \tilde{\mathbf{w}}; p)$:

$$\hat{\tau}_{i,t}(\mathbf{w}, \tilde{\mathbf{w}}; p) := \left\{ \frac{Y_{i,t}(w_{i,1:t-p-1}^{obs}, \mathbf{w}) \mathbb{1}(w_{i,t-p:t}^{obs} = \mathbf{w})}{p_{i,t-p}(\mathbf{w})} - \frac{Y_{i,t}(w_{i,1:t-p-1}^{obs}, \tilde{\mathbf{w}}) \mathbb{1}(w_{i,t-p:t}^{obs} = \tilde{\mathbf{w}})}{p_{i,t-p}(\tilde{\mathbf{w}})} \right\}, \quad (3)$$

where $\mathbb{1}\{A\}$ is an indicator function taking the value 1 if A is true and 0 otherwise. We show below that this estimator is conditionally unbiased for the i, t -th lag- p dynamic causal effect over the treatment path assignment mechanism, with a simple conditional covariance.

Crucially, under non-interference (Assumption 5), the estimator simplifies to

$$\hat{\tau}_{i,t}(\mathbf{w}, \tilde{\mathbf{w}}; p) = \frac{y_{i,t}^{obs} \{ \mathbb{1}(w_{i,t-p:t}^{obs} = \mathbf{w}) - \mathbb{1}(w_{i,t-p:t}^{obs} = \tilde{\mathbf{w}}) \}}{p_{i,t-p}(w_{i,t-p:t}^{obs})}, \quad (4)$$

which is computable as $p_{i,t-p}(w_{i,t-p:t}^{obs})$ is available by construction.

Theorem 3.1. *Consider a potential outcome panel that satisfies non-interfering probabilistic treatment assignment (Assumptions 5 and 6). For any $\mathbf{w}, \tilde{\mathbf{w}} \in \mathcal{W}^{(p+1)}$,*

$$\mathbb{E}[\hat{\tau}_{i,t}(\mathbf{w}, \tilde{\mathbf{w}}; p) | \mathcal{F}_{i,t-p-1}] = \tau_{i,t}(\mathbf{w}, \tilde{\mathbf{w}}; p), \quad (5)$$

$$Var(\hat{\tau}_{i,t}(\mathbf{w}, \tilde{\mathbf{w}}; p) | \mathcal{F}_{i,t-p-1}) = \gamma_{i,t}^2(\mathbf{w}, \tilde{\mathbf{w}}) - \tau_{i,t}(\mathbf{w}, \tilde{\mathbf{w}}; p)^2, \quad (6)$$

where

$$\gamma_{i,t}^2(\mathbf{w}, \tilde{\mathbf{w}}; p) = \frac{Y_{i,t}(w_{i,1:t-p-1}^{obs}, \mathbf{w})^2}{p_{i,t-p}(\mathbf{w})} + \frac{Y_{i,t}(w_{i,1:t-p-1}^{obs}, \tilde{\mathbf{w}})^2}{p_{i,t-p}(\tilde{\mathbf{w}})}. \quad (7)$$

Further, for distinct $\mathbf{w}, \tilde{\mathbf{w}}, \bar{\mathbf{w}}, \hat{\mathbf{w}} \in \mathcal{W}^{(p+1)}$

$$Cov(\hat{\tau}_{i,t}(\mathbf{w}, \tilde{\mathbf{w}}; p), \hat{\tau}_{i,t}(\bar{\mathbf{w}}, \hat{\mathbf{w}}; p) | \mathcal{F}_{i,t-p-1}) = -\tau_{i,t}(\mathbf{w}, \tilde{\mathbf{w}}; p)\tau_{i,t}(\bar{\mathbf{w}}, \hat{\mathbf{w}}; p).$$

Finally, under non-interference, $\hat{\tau}_{i,t}(\mathbf{w}, \tilde{\mathbf{w}})$ and $\hat{\tau}_{j,t}(\mathbf{w}, \tilde{\mathbf{w}})$ are independent for $i \neq j$ conditional on $\mathcal{F}_{1:N, t-p-1}$,

Proof. Given in the Appendix. \square

Theorem 3.1 states that for every i, t , the error in estimating $\tau_{i,t}(\mathbf{w}, \tilde{\mathbf{w}}; p)$ is a martingale difference sequence (e.g., Hall and Heyde (1980)) through time and conditionally independent over the cross-section. As is common in potential outcome frameworks, the variance of $\hat{\tau}_{i,t}(\mathbf{w}, \tilde{\mathbf{w}}; p)$ depends upon the potential outcomes under both the treatment and counterfactual (e.g. see Imbens and Rubin (2015) and Ding (2017)) and is generally not estimable. However, as shown in Theorem 3.1, the variance is bounded from above by $\gamma_{i,t}^2(\mathbf{w}, \tilde{\mathbf{w}}; p)$, which we can estimate by

$$\hat{\gamma}_{i,t}^2(\mathbf{w}, \tilde{\mathbf{w}}; p) = \frac{(y_{i,t}^{obs})^2 \{\mathbb{1}(w_{i,t-p:t}^{obs} = \mathbf{w}) + \mathbb{1}(w_{i,t-p:t}^{obs} = \tilde{\mathbf{w}})\}}{p_{i,t-p}(w_{i,t-p:t}^{obs})^2}. \quad (8)$$

The following lemma establishes that $\hat{\gamma}_{i,t}^2(\mathbf{w}, \tilde{\mathbf{w}}; p)$ is an unbiased estimator of $\gamma_{i,t}^2(\mathbf{w}, \tilde{\mathbf{w}}; p)$.

Lemma 3.2. *Under the set up of Theorem 3.1,*

$$\mathbb{E}[\hat{\gamma}_{i,t}^2(\mathbf{w}, \tilde{\mathbf{w}}; p) | \mathcal{F}_{i,t-p-1}] = \gamma_{i,t}^2(\mathbf{w}, \tilde{\mathbf{w}}; p)$$

Therefore, since $\hat{\gamma}_{i,t}^2(\mathbf{w}, \tilde{\mathbf{w}}; p)$ is an unbiased estimator of the conservative variance, $\gamma_{i,t}^2(\mathbf{w}, \tilde{\mathbf{w}})$, it is possible to carry out nonparametric conservative inference.

Remark 3.2. *Since the weighted average i, t -th lag- p, q dynamic causal effects (Definition 6) are linear combinations of the i, t -th lag- p dynamic causal effects, we can directly apply Theorem 3.1 and Lemma 3.2. We provide the details for the case when $q = 1$.*

A feasible nonparametric estimator of

$$\tau_{i,t}^\dagger(w, \tilde{w}; p) = \sum_{\mathbf{v} \in W^p} a_{\mathbf{v}} \left\{ Y_{i,t}(w_{i,1:t-p-1}^{obs}, w, \mathbf{v}) - Y_{i,t}(w_{i,1:t-p-1}^{obs}, \tilde{w}, \mathbf{v}) \right\},$$

where $w, \tilde{w} \in \mathcal{W}$ and $\mathbf{v} \in \mathcal{W}^p$ is

$$\hat{\tau}_{i,t}^\dagger(w, \tilde{w}; p) = \sum_{\mathbf{v} \in W^p} a_{\mathbf{v}} \left\{ \frac{Y_{i,t}(w_{i,1:t-p-1}^{obs}, w, \mathbf{v}) \mathbb{1}(w_{i,t-p:t}^{obs} = (w, \mathbf{v}))}{p_{i,t-p}(w, \mathbf{v})} - \frac{Y_{i,t}(w_{i,1:t-p-1}^{obs}, \tilde{w}, \mathbf{v}) \mathbb{1}(w_{i,t-p:t}^{obs} = (\tilde{w}, \mathbf{v}))}{p_{i,t-p}(\tilde{w}, \mathbf{v})} \right\}.$$

Under non-interference, we can again simplify this to,

$$\hat{\tau}_{i,t}^\dagger(w, \tilde{w}; p) = \frac{a_{w_{i,t-p+1:t}^{obs}} y_{i,t}^{obs} \{ \mathbb{1}(w_{i,t-p}^{obs} = w) - \mathbb{1}(w_{i,t-p}^{obs} = \tilde{w}) \}}{p_{i,t-p}(w_{i,t-p:t}^{obs})}.$$

Again, this estimator is unbiased, over the randomization distribution, with variance that can be bounded from above. For uniform weights, the rest of the generalizations follow immediately by noticing that we can replace all instances of \mathbf{w} and $\tilde{\mathbf{w}}$ with (\mathbf{w}, \mathbf{v}) and $(\tilde{\mathbf{w}}, \mathbf{v})$. Without uniform weights, the notation becomes cumbersome, but there are no substantive changes.

3.3 Estimation of lap- p average treatment effects

The martingale difference properties of the nonparametric estimator means that the cross-sectional and temporally averaged estimators

$$\hat{\tau}_t(\mathbf{w}, \tilde{\mathbf{w}}; p) := \frac{1}{N} \sum_{i=1}^N \hat{\tau}_{i,t}(\mathbf{w}, \tilde{\mathbf{w}}; p) \tag{9}$$

$$\hat{\tau}_i(\mathbf{w}, \tilde{\mathbf{w}}; p) := \frac{1}{(T-p)} \sum_{t=p+1}^T \hat{\tau}_{i,t}(\mathbf{w}, \tilde{\mathbf{w}}; p) \tag{10}$$

$$\hat{\tau}(\mathbf{w}, \tilde{\mathbf{w}}; p) := \frac{1}{N(T-p)} \sum_{i=1}^N \sum_{t=p+1}^T \hat{\tau}_{i,t}(\mathbf{w}, \tilde{\mathbf{w}}; p) \tag{11}$$

are also unbiased estimators of the average causal estimands $\bar{\tau}_t(\mathbf{w}, \tilde{\mathbf{w}}; p)$, $\bar{\tau}_i(\mathbf{w}, \tilde{\mathbf{w}}; p)$ and $\bar{\tau}(\mathbf{w}, \tilde{\mathbf{w}}; p)$, respectively.

Moreover, the martingale difference properties greatly ease the calculation of variances of cross-sectional and temporal averages, and allow us to apply a central limit theorem to appropriately scaled

and centered versions of these estimators. In particular, write:

$$\sigma_t^2 := \frac{1}{N} \sum_{i=1}^N \{\gamma_{i,t}^2(\mathbf{w}, \tilde{\mathbf{w}}) - \tau_{i,t}(\mathbf{w}, \tilde{\mathbf{w}}; p)^2\} \quad (12)$$

$$\sigma_i^2 := \frac{1}{(T-p)} \sum_{t=p+1}^T \{\gamma_{i,t}^2(\mathbf{w}, \tilde{\mathbf{w}}) - \tau_{i,t}(\mathbf{w}, \tilde{\mathbf{w}}; p)^2\}, \quad (13)$$

$$\sigma^2 := \frac{1}{N(T-p)} \sum_{i=1}^N \sum_{t=p+1}^T \{\gamma_{i,t}^2(\mathbf{w}, \tilde{\mathbf{w}}) - \tau_{i,t}(\mathbf{w}, \tilde{\mathbf{w}}; p)^2\}. \quad (14)$$

Theorem 3.2. *Consider a potential outcome panel that satisfies non-interfering probabilistic treatment assignment (Assumptions 5 and 6). Further assume that the potential outcomes are bounded. Then, for any $\mathbf{w}, \tilde{\mathbf{w}} \in \mathcal{W}^{(p+1)}$,*

$$\begin{aligned} \frac{\sqrt{N}\{\hat{\tau}_t(\mathbf{w}, \tilde{\mathbf{w}}; p) - \bar{\tau}_t(\mathbf{w}, \tilde{\mathbf{w}}; p)\}}{\sigma_t} &\xrightarrow{d} N(0, 1) \quad \text{as } N \rightarrow \infty, \\ \frac{\sqrt{T-p}\{\hat{\tau}_i(\mathbf{w}, \tilde{\mathbf{w}}; p) - \bar{\tau}_i(\mathbf{w}, \tilde{\mathbf{w}}; p)\}}{\sigma_i} &\xrightarrow{d} N(0, 1) \quad \text{as } T \rightarrow \infty, \\ \frac{\sqrt{N(T-p)}\{\hat{\tau}(\mathbf{w}, \tilde{\mathbf{w}}; p) - \bar{\tau}(\mathbf{w}, \tilde{\mathbf{w}}; p)\}}{\sigma} &\xrightarrow{d} N(0, 1) \quad \text{as } NT \rightarrow \infty. \end{aligned}$$

Proof. Given in the Appendix. \square

Likewise, for bounded potential outcomes with non-interfering, probabilistic treatment assignments, the scaled variances are, exactly, equal to

$$N \times \text{Var}(\hat{\tau}_t(w, \tilde{w}; p) | \mathcal{F}_{1:N, t-p-1}) = \mathbb{E}[\sigma_t^2 | \mathcal{F}_{1:N, t-p-1}], \quad (15)$$

$$(T-p) \times \text{Var}(\hat{\tau}_i(w, \tilde{w}; p) | \mathcal{F}_{i,0}) = \mathbb{E}[\sigma_i^2 | \mathcal{F}_{i,0}], \quad (16)$$

$$N(T-p) \times \text{Var}(\hat{\tau}(w, \tilde{w}; p) | \mathcal{F}_{1:N,0}) = \mathbb{E}[\sigma^2 | \mathcal{F}_{1:N,0}]. \quad (17)$$

Following the same logic as earlier, we can establish unbiased estimators of an upper-bound for the variance. We do so in the next lemma, establishing feasible, unbiased estimators for upper-bounds on σ_t^2 , σ_i^2 and σ^2 .

Lemma 3.3. *Under the set up of Theorem 3.2,*

$$\begin{aligned}\mathbb{E} \left[\frac{1}{N} \sum_{i=1}^N \hat{\gamma}_{i,t}^2(\mathbf{w}, \tilde{\mathbf{w}}; p) \mid \mathcal{F}_{1:N, t-p-1} \right] &= \frac{1}{N} \sum_{i=1}^N \gamma_{i,t}^2(\mathbf{w}, \tilde{\mathbf{w}}; p), \\ \mathbb{E} \left[\frac{1}{(T-p)} \sum_{t=p+1}^T \hat{\gamma}_{i,t}^2(\mathbf{w}, \tilde{\mathbf{w}}; p) \mid \mathcal{F}_{i,0} \right] &= \frac{1}{(T-p)} \sum_{t=p+1}^T \gamma_{i,t}^2(\mathbf{w}, \tilde{\mathbf{w}}; p), \\ \mathbb{E} \left[\frac{1}{N(T-p)} \sum_{i=1}^N \sum_{t=p+1}^T \hat{\gamma}_{i,t}^2(\mathbf{w}, \tilde{\mathbf{w}}; p) \mid \mathcal{F}_{1:N, 0} \right] &= \frac{1}{N(T-p)} \sum_{i=1}^N \sum_{t=p+1}^T \gamma_{i,t}^2(\mathbf{w}, \tilde{\mathbf{w}}; p),\end{aligned}$$

The results in Theorem 3.2 and Lemma 3.3 naturally extend to the weighted average i, t -th lag- p, q dynamic causal effect from Definition 6 by using the estimator developed in Remark 3.2.

Remark 3.3. *Theorem 3.2 shows that for panel experiments, we can increase the precision not only by increasing the sample size but also by increasing the duration of the experiment. This result is appealing because, in some settings, it may be hard or impossible to increase the number of participants. At the same time, it may be easy to increase the duration of the experiment. In Section 5, we explore this insight through a simulation study.*

3.4 Confidence intervals and testing for lap- p average treatment effects

Combining the estimators in Lemma (3.3) with the central limit theorems in Theorem 3.2, we can carry out conservative inference for $\bar{\tau}_t(\mathbf{w}, \tilde{\mathbf{w}}; p)$, $\bar{\tau}_i(\mathbf{w}, \tilde{\mathbf{w}}; p)$ and $\bar{\tau}(\mathbf{w}, \tilde{\mathbf{w}}; p)$. Such inference techniques can be used to provide asymptotic conservative confidence intervals or to carry out asymptotic hypothesis testing of a Neyman-type, weak nulls that the average dynamic causal effects are zero. For example, these may be $H_0 : \bar{\tau}_i(\mathbf{w}, \tilde{\mathbf{w}}; p) = 0$ for $i = 3$ or $H_0 : \bar{\tau}_t(\mathbf{w}, \tilde{\mathbf{w}}; p) = 0$ for $t = 4$. Of course, each of these test carries different interpretations and finding the appropriate null hypothesis is up to the practitioner.

An alternative is the more stringent Fisher-type, sharp nulls. An example of this would be $H_0 : \bar{\tau}_{i,t}(\mathbf{w}, \tilde{\mathbf{w}}; p) = 0$, for all $i \in [N]$ and specific $t = 4$. The key feature of the Fisher-type null is that it reveals all the potential outcomes $Y_{i,t}(w_{1:t-p-1}^{obs}, w) = y_{i,t}^{obs}$ for all w and i . Hence we can simulate for each i , the treatment path $W_{i,t-p:t} | W_{i,1:t-p-1}^{obs}, y_{i,1:t-p-1}^{obs}$ and then compute the corresponding $\hat{\tau}_{i,t}(\mathbf{w}, \tilde{\mathbf{w}}; p)$. This allows the exact distribution of $\hat{\tau}_t(\mathbf{w}, \tilde{\mathbf{w}}; p)$ to be simulated under the null and, by comparing it to the observed one, allows us to compute an exact p -value. Tests of these Fisher nulls

can be inverted to provide confidence intervals for $\bar{\tau}_i(\mathbf{w}, \tilde{\mathbf{w}}; p)$.

4 Estimation in a linear potential outcome panel

Much of the existing literature on causal inference from panel data in econometrics focuses on using linear models that assume the outcome is a linear function of the treatment path. In this section, we explore the properties of such standard methods for estimating causal coefficients in a linear potential outcome panel when there exists a dynamic causal effects. We begin by analyzing a panel experiment as a repeated cross-section, estimating a separate linear model with the data in each period. We then consider the canonical unit fixed-effects estimator and two-way fixed effects estimator, highlighting the bias induced by the presence of dynamic causal effects. Following convention, we derive the probability limit of each estimator as the number of units N grows large, holding the number of periods T fixed.

4.1 Estimation as a repeated cross-section

First, we analyze the panel experiment as a repeated cross-section, estimating a separate linear model in each period t under the assumption of homogeneous, linear potential outcomes. The available data at time t are the entire treatment panel $W_{1:N,1:t}$ and the observed outcomes $Y_{1:N,1:t}(W_{1:N,1:t})$. Denote the within-period transformed data as $\dot{Y}_{i,t} = Y_{i,t} - \bar{Y}_t$, $\dot{W}_{i,t} = (W_{i,t} - \bar{W}_t, W_{i,t-1} - \bar{W}_{t-1}, \dots, W_{i,1} - \bar{W}_1)'$ and write $\dot{Y}_{1:N,t} = (\dot{Y}_{1,t}, \dots, \dot{Y}_{N,t})'$ and $\dot{W}_{1:N,t} = (\dot{W}_{1,t}, \dots, \dot{W}_{N,t})'$. The least squares coefficient in the regression of \dot{Y} on \dot{W}_t is then $\hat{\beta}_{1:N,t} = (\dot{W}_{1:N,t}' \dot{W}_{1:N,t})^{-1} \dot{W}_{1:N,t}' \dot{Y}_{1:N,t}$.

Proposition 4.1 derives the finite population limiting distribution of $\hat{\beta}_{1:N,t}$ as the number of units grows large.

Proposition 4.1. *Assume a potential outcome panel and consider the “control” only path, for $0 \in \mathcal{W}$ let $\tilde{w}_{i,1:t} = \mathbf{0}$. Define the error $\dot{v}_{i,t}(\mathbf{0}) = Y_{i,t}(\mathbf{0}) - \bar{Y}_t(\mathbf{0})$, with $\bar{Y}_t(\mathbf{0}) = \frac{1}{N} \sum_{i=1}^N Y_{i,t}(\mathbf{0})$. Let $\dot{\mu}_{i,t}$ be the $t \times 1$ vector whose u -th element is $E[\dot{W}_{i,t-(u-1)} | \mathcal{F}_{1:N,0,T}]$ and $\Omega_{i,t}$ be the $t \times t$ matrix whose u, v -th element is $Cov(\dot{W}_{i,t-(u-1)}, \dot{W}_{i,t-(v-1)} | \mathcal{F}_{1:N,0,T})$. Additionally assume that:*

1. *The potential outcome panel is linear and homogeneous (Definitions 3-4).*
2. *$W_{i,1:t}$ is a non-interfering stochastic treatment path and, over the randomization distribution, $Var(W_{i,t} | \mathcal{F}_{1:N,0,T}) = \sigma_{W,i,t}^2 < \infty$ for each $i \in [N]$, $t \in [T]$.*

3. As $N \rightarrow \infty$,

- (a) Non-stochastically, $N^{-1} \sum_{i=1}^N \Omega_{i,t} \rightarrow \Gamma_{2,t}$, where $\Gamma_{2,t}$ is positive definite.
- (b) $N^{-1/2} \sum_{i=1}^N (\dot{W}_{i,t} - \dot{\mu}_{i,t}) \dot{\nu}_{i,t}(\mathbf{0}) | \mathcal{F}_{1:N,0,T} \xrightarrow{d} N(0, \Gamma_{1,t})$.
- (c) Non-stochastically, $N^{-1} \sum_{i=1}^N \dot{\nu}_{i,t}(\mathbf{0}) \dot{\mu}_{i,t} \rightarrow \dot{\delta}_t$.

Then, over the randomization distribution, as $N \rightarrow \infty$,

$$\sqrt{N}(\hat{\beta}_t - \beta_t - \Gamma_{2,t}^{-1} \dot{\delta}_t) | \mathcal{F}_{1:N,0,T} \xrightarrow{d} N(0, \Gamma_{2,t}^{-1} \Gamma_{1,t} \Gamma_{2,t}^{-1}).$$

Proof. Given in the Appendix. \square

Typically we might expect that the asymptotic bias induced by $\Gamma_{2,t}^{-1} \dot{\delta}_t$ to be zero, as the deviations of the counterfactual for unit- i at time- t is unlikely to covary with the path of the expected treatment, given we are conditioning on the potential outcomes. However, this condition needs to be checked depending on the particular treatment assignment mechanism.

4.2 Interpreting the unit fixed effects estimator

Researchers often estimate linear models with unit fixed effects in panel data. Define the within-unit transformed data, $\check{Y}_{i,t} = Y_{i,t} - \bar{Y}_i$, and $\check{W}_{i,t} = W_{i,t} - \bar{W}_i$. Then, the unit fixed effect estimator is $\hat{\beta}_{UFE} = \sum_{i=1}^N \sum_{t=1}^T \check{Y}_{i,t} \check{W}_{i,t} / \sum_{i=1}^N \sum_{t=1}^T \check{W}_{i,t}^2$. Our next result characterizes the finite population probability limit of the unit fixed estimator as N grows large, allowing for arbitrary heterogeneity in the causal coefficients across units and time periods.

Proposition 4.2. *Assume a potential outcome panel and consider the “control” only path, for $0 \in \mathcal{W}$ let $\tilde{w}_{i,1:t} = \mathbf{0}$. Denote $\check{\nu}_{i,t}(\mathbf{0}) = Y_{i,t}(\mathbf{0}) - \bar{Y}_i(\mathbf{0})$, $Cov(\check{W}_{i,t}, \check{W}_{i,s}) = \check{\sigma}_{W,i,t,s}$ and $\check{\mu}_{i,t} = \mathbb{E}[\check{W}_{i,t} | \mathcal{F}_{1:N,0,T}]$. Additionally, assume the potential outcome panel is linear (Definition 3), the treatment assignment mechanism is non-interfering and $Var(\check{W}_{i,t} | \mathcal{F}_{1:N,0,T}) = \check{\sigma}_{W,i,t}^2 < \infty$ for each $i \in [N]$, $t \in [T]$. Further assume that as $N \rightarrow \infty$, the following sequences converge non-stochastically:*

$$\begin{aligned} N^{-1} \sum_{i=1}^N \beta_{i,t,s} \check{\sigma}_{W,i,t,s} &\rightarrow \check{\kappa}_{W,\beta,t,s} \quad \forall t \in [T] \& s \leq t, \\ N^{-1} \sum_{i=1}^N \check{\sigma}_{W,i,t}^2 &\rightarrow \check{\sigma}_{W,t}^2 \quad \forall t \in [T], \end{aligned}$$

$$N^{-1} \sum_{i=1}^N \tilde{\nu}_{i,t}(\mathbf{0}) \tilde{\mu}_{i,t} \rightarrow \check{\delta}_t \quad \forall t \in [T].$$

Then, as $N \rightarrow \infty$,

$$\hat{\beta}_{UFE} \xrightarrow{p} \frac{\sum_{t=1}^T \check{\kappa}_{W,\beta,t,t}}{\sum_{t=1}^T \check{\sigma}_{W,t}^2} + \frac{\sum_{t=1}^T \sum_{s=1}^{t-1} \check{\kappa}_{W,\beta,t,s}}{\sum_{t=1}^T \check{\sigma}_{W,t}^2} + \frac{\sum_{t=1}^T \check{\delta}_t}{\sum_{t=1}^T \check{\sigma}_{W,t}^2}. \quad (18)$$

Proof. Given in the Appendix. \square

Proposition 4.2 decomposes the finite population probability limit of the unit fixed effects estimator into three terms. The first term is an average of contemporaneous dynamic causal coefficients, describing how the contemporaneous causal coefficients covary with the within-unit transformed treatments over the treatment assignment mechanism. The second term captures how past causal coefficients covary with the within-unit transformed treatments and arises due to the presence of dynamic causal effects. The last term is an additional error that arises due to the possible relationship between the demeaned counterfactual $\nu_{i,t}(\mathbf{0})$ and the average, demeaned treatment assignment.

To highlight the intuition of this result, we consider a simple example.

Example 8. Consider an autoregressive potential outcome panel model (Example 1) with

$$Y_{i,t}(w_{i,1:t}) = \beta_0 w_{i,t} + \beta_1 w_{i,t-1} + \epsilon_{i,t} \quad \forall t > 1,$$

$$Y_{i,1}(w_{i,1}) = \beta_0 w_{i,1} + \epsilon_{i,1}.$$

That is, there is no heterogeneity across units or time periods in the causal effects and no persistence.

In this simple case, Proposition 4.2 implies

$$\hat{\beta}_{UFE} = \beta_0 + \beta_1 \frac{\sum_{t=2}^T \sigma_{\check{W},t,t-1}}{\sum_{t=1}^T \sigma_{\check{W},t}^2} + \frac{\sum_{t=1}^T \check{\delta}_t}{\sum_{t=1}^T \sigma_{\check{W},t}^2}.$$

In other words, the unit fixed effects estimator converges in probability to the contemporaneous dynamic causal coefficient β_0 plus a bias that depends on two terms. The first component of the bias depends on the lag-1 dynamic causal coefficient and the average covariance between the treatments across periods – if there is serial correlation in the treatment assignment mechanism across periods, this term will be non-zero.

4.3 Interpreting the two-way fixed effects estimator

Finally, we analyze the finite population probability limit of the two-way fixed effects estimator using the linear potential outcome panel model. It is increasingly common for researchers to estimate linear models with both unit and time fixed effects in panel data.¹⁰ For a generic variable $W_{i,t}$, denote the unit and time demeaned variable $\dot{\bar{X}}_{i,t} = (X_{i,t} - \bar{X}) - (\bar{X}_t - \bar{X}) - (\bar{X}_i - \bar{X})$. The two-way fixed-effect estimator is then defined as $\hat{\beta}_{TWFE} = \sum_{i=1}^N \sum_{t=1}^T \dot{\bar{Y}}_{i,t} \dot{\bar{W}}_{i,t} / \sum_{i=1}^N \sum_{t=1}^T \dot{\bar{W}}_{i,t}^2$. For example, [Sobel \(2006\)](#), [Athey and Imbens \(2018\)](#), and [Imai and Kim \(2019a\)](#) study $\hat{\beta}_{TWFE}$ in the causal literature on panel data models.

We derive the finite population probability limit of the two-way fixed effects estimator under the assumption of additive causal effects, allowing for arbitrary heterogeneity across units and time periods and holding T fixed as $N \rightarrow \infty$.

Proposition 4.3. *Assume a potential outcome panel and consider the “control” only path, for $0 \in \mathcal{W}$ let $\tilde{w}_{i,1:t} = \mathbf{0}$. Denote $\dot{\tilde{\nu}}_{i,t}(\mathbf{0}) = \dot{\bar{Y}}_{i,t}(\mathbf{0})$, $E(\dot{\bar{W}}_{i,t} | \mathcal{F}_{1:N,0,T}) = \dot{\tilde{\mu}}_{i,t}$ and $Cov(\dot{\bar{W}}_{i,t}, \dot{\bar{W}}_{i,s}) = \dot{\tilde{\sigma}}_{W,i,t,s}$. Additionally, assume that the potential outcome panel is linear (Definition 3), the treatment assignment mechanism is non-interfering and $Var(\dot{\bar{W}}_{i,t} | \mathcal{F}_{1:N,0,T}) = \dot{\tilde{\sigma}}_{W,i,t}^2 < \infty$ for each $i \in [N]$, $t \in [T]$. Further assume that as $N \rightarrow \infty$, the following sequences converge non-stochastically*

$$\begin{aligned} N^{-1} \sum_{i=1}^N \beta_{i,t,s} \dot{\tilde{\sigma}}_{W,i,t,s} &\rightarrow \dot{\tilde{\kappa}}_{W,\beta,t,s} \quad \forall t \in [T] \& s \leq t, \\ N^{-1} \sum_{i=1}^N \dot{\tilde{\sigma}}_{W,i,t}^2 &\rightarrow \dot{\tilde{\sigma}}_{W,t}^2 \quad \forall t \in [T], \\ N^{-1} \sum_{i=1}^N \dot{\tilde{\nu}}_{i,t}(\mathbf{0}) \dot{\tilde{\mu}}_{i,t} &\rightarrow \dot{\tilde{\delta}}_t \quad \forall t \in [T]. \end{aligned}$$

Then, as $N \rightarrow \infty$,

$$\hat{\beta}_{TWFE} \xrightarrow{p} \frac{\sum_{t=1}^T \dot{\tilde{\kappa}}_{W,\beta,t,t}}{\sum_{t=1}^T \dot{\tilde{\sigma}}_{W,t}^2} + \frac{\sum_{t=1}^T \sum_{s=1}^{t-1} \dot{\tilde{\kappa}}_{W,\beta,t,s}}{\sum_{t=1}^T \dot{\tilde{\sigma}}_{W,t}^2} + \frac{\sum_{t=1}^T \dot{\tilde{\delta}}_t}{\sum_{t=1}^T \dot{\tilde{\sigma}}_{W,t}^2}$$

Proof. Given in the Appendix. □

¹⁰This is often referred to as the “static” or “canonical” two-way fixed effects specification (e.g. [Boryusak and Jaravel \(2017\)](#) and [Allegretto et al. \(2017\)](#)). A recent active area of research focuses on interpreting the “dynamic” two-way fixed effects, which additionally includes leads and lags of the treatment. See, for example, [de Chaisemartin and D’Haultfoeuille \(2019\)](#), [Abraham and Sun \(2019\)](#) and [Hull \(2018\)](#).

Similar to our result for the unit fixed effects estimator, Proposition 4.3 shows that the two-way fixed effects estimand decomposes into three components under additive causal effects, where the interpretation of each component is similar to the unit fixed effects estimator.

5 Simulation Study

We now conduct a simulation study to investigate the finite sample properties of the asymptotic results presented in Section 3. We show that the finite population central limit theorems (Theorem 3.2) hold for a moderate number of treatment periods and experimental units. The proposed conservative tests also have correct size under the weak null of no average dynamic causal effects and reasonable rejection rates against a range of alternatives.

5.1 Simulation design

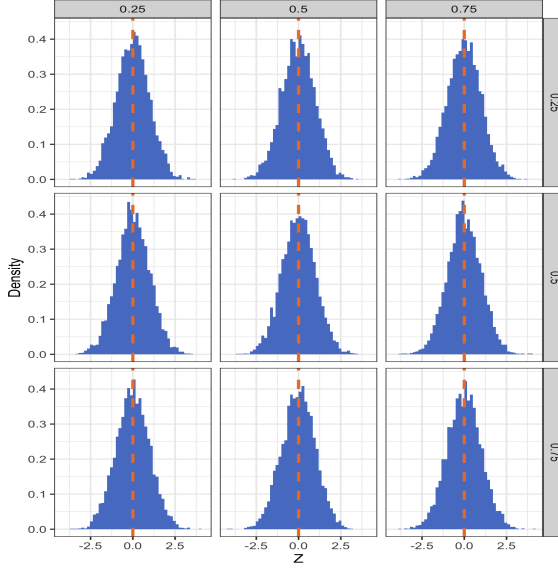
Throughout the simulation we generate the panel experiment using the autoregressive potential outcome panel model from Example 1,

$$Y_{i,t} = \phi_{i,t,0} Y_{i,t-1}(w_{i,1:t-1}) + \dots + \phi_{i,t,t-2} Y_{i,1}(w_{i,1}) + \beta_{i,t,0} w_{i,t} + \dots + \beta_{i,t,t-1} w_{i,1} + \epsilon_{i,t} \quad \forall t > 1,$$

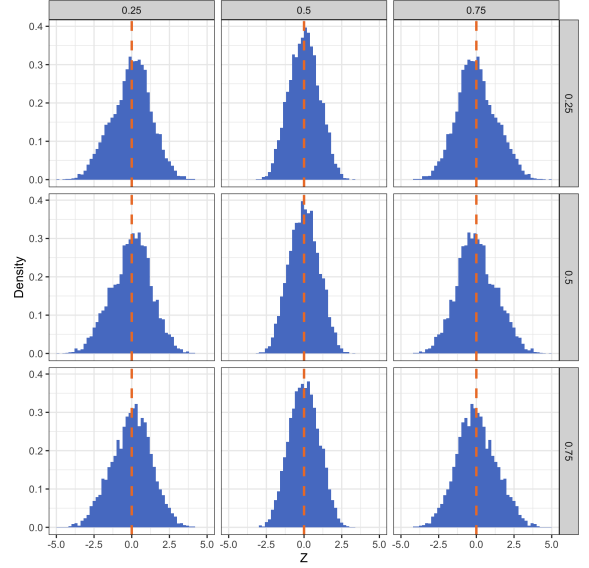
$$Y_{i,1}(w_{i,1}) = \beta_{i,1,0} w_{i,1} + \epsilon_{i,1},$$

with $\phi_{i,t,0} \equiv \phi$, $\phi_{i,t,s} \equiv 0$ for $s > 0$, $\beta_{i,t,0} \equiv \beta$ and $\beta_{i,t,s} \equiv 0$ for $s > 0$. We vary the choice ϕ , which governs the persistence of the process, and β , which governs the size of the contemporaneous causal effects. We also vary the probability of treatment $p_{i,t-p}(w) = p(w)$ as well as the distribution of the errors ϵ_i , which we will either sample from a standard normal or a Cauchy distribution.

In all simulations, we document the performance of our nonparametric estimators over the randomization distribution, meaning that we first generate the potential outcomes $Y_{1:N,1:T}(\bullet)$ and then, holding these fixed, simulate over different treatment panels $W_{1:N,1:T}$.



(a) $\epsilon_{i,t} \sim N(0, 1)$, $N = 1000$



(b) $\epsilon_{i,t} \sim \text{Cauchy}$, $N = 50,000$

Figure 1: Simulated randomization distribution for $\hat{\tau}_t(1, 0; 0)$ under different choices of the parameter ϕ (defined in Example 1) and treatment probability $p(w)$. The rows index the parameter ϕ , which ranges over values $\{0.25, 0.5, 0.75\}$. The columns index the treatment probability $p(w)$, which ranges over values $\{0.25, 0.5, 0.75\}$. Panel (a) plots the simulated randomization distribution with normally distributed errors $\epsilon_{i,t} \sim N(0, 1)$ and $N = 1000$. Panel (b) plots the simulated randomization distribution with Cauchy distribution errors $\epsilon_{i,t} \sim \text{Cauchy}$ and $N = 50,000$. Results are computed over 5,000 iterations.

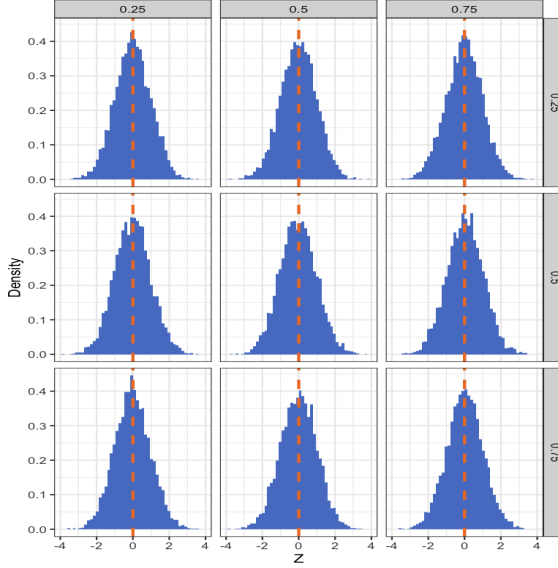
5.2 Simulation results

5.2.1 Normal approximations and size control

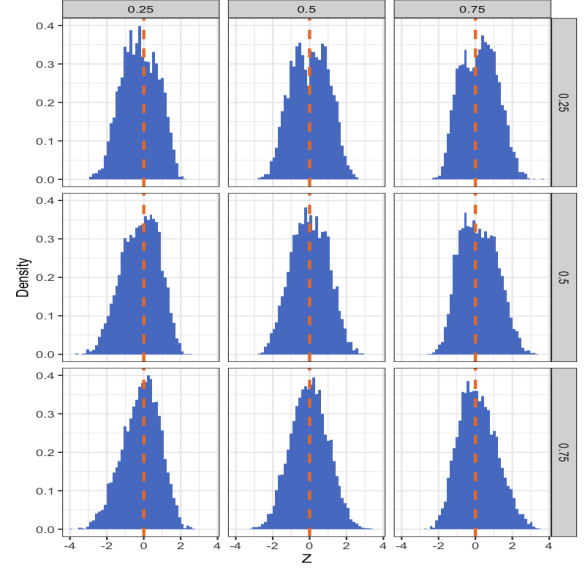
Figure 1 plots the randomization distribution for $\hat{\tau}_t(1, 0; 0)$ under the null hypothesis of $\beta = 0$ for different combinations of the parameter $\phi \in \{0.25, 0.5, 0.75\}$ and treatment probability $p(w) \in \{0.25, 0.5, 0.75\}$. When the errors $\epsilon_{i,t}$ are normally distributed, the randomization distribution quickly converges to a normal distribution. As expected, when the errors are Cauchy distributed, the number of units must be quite large for the the randomization distribution to become approximately normal. There is little difference in the results across the values of ϕ and $p(w)$.

Testing based on the normal asymptotic approximation controls size effectively, staying close to the nominal 5% level (the exact rejection rates for the null hypothesis, $H_0 : \bar{\tau}_t(1, 0; 0) = 0$ are reported in Table A1).

Figure 2 plots the randomization distribution for $\hat{\tau}_i(1, 0; 0)$. We see a similar pattern as before—when the errors are normally distributed, the randomization distribution converges quickly to a normal distribution, but it takes longer to do so when the errors are heavy-tailed. Again, the null rejection



(a) $\epsilon_{i,t} \sim N(0, 1)$, $T = 1000$



(b) $\epsilon_{i,t} \sim \text{Cauchy}$, $T = 50,000$

Figure 2: Simulated randomization distribution for $\hat{\tau}_i^\dagger(1, 0; 0)$ under different choices of the parameter ϕ (defined in Example 1) and treatment probability $p(w)$. The rows index the parameter ϕ , which ranges over values $\{0.25, 0.5, 0.75\}$. The columns index the treatment probability $p(w)$, which ranges over values $\{0.25, 0.5, 0.75\}$. Panel (a) plots the simulated randomization distribution with normally distributed errors $\epsilon_{i,t} \sim N(0, 1)$ and $T = 1000$. Panel (b) plots the simulated randomization distribution with Cauchy distribution errors $\epsilon_{i,t} \sim \text{Cauchy}$ and $T = 50,000$. Results are computed over 5,000 simulations.

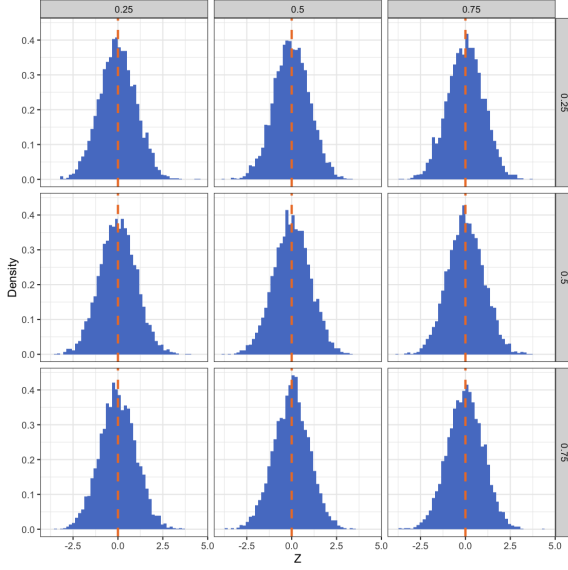
rates for the null hypothesis, $H_0 : \bar{\tau}_i(1, 0; 0) = 0$ are reported in Table A2 and the test controls size well across a wide range of parameters.

Figure 3 plots the randomization distribution for $\hat{\tau}^\dagger(1, 0; 1)$. We present results for the case with $N = 100$, $T = 10$ and $N = 500$, $T = 100$ but note that the results are similar when the roles of N, T are reversed. The null rejection rates for the null hypothesis, $H_0 : \hat{\tau}^\dagger(1, 0; 1) = 0$ are reported in Table A3.

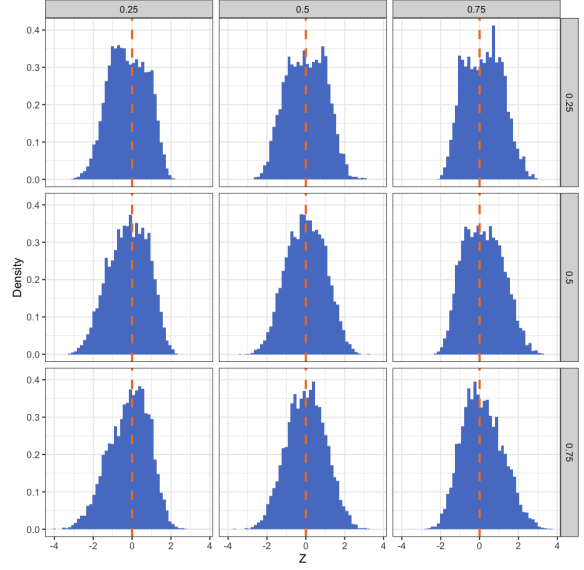
Figures A1-A3 in the Appendix provides quantile-quantile plots of the simulated randomization distributions to further illustrate the quality of the normal approximations. We also plot the randomization distributions for $\hat{\tau}_t^\dagger(1, 0; 1)$, $\hat{\tau}_i^\dagger(1, 0; 1)$ and $\hat{\tau}^\dagger(1, 0; 1)$ in Figures A4-A6 respectively.

5.2.2 Rejection rate

Focusing on simulations with normally distributed errors, we next investigate the rejection rate of statistical tests based on the normal asymptotic approximations. To do so, we generate potential outcomes $Y_{1:N, 1:T}(\bullet)$ under different values of β , which governs the magnitude of the contemporaneous



(a) $\epsilon_{i,t} \sim N(0, 1)$, $N = 100$, $T = 10$



(b) $\epsilon_{i,t} \sim \text{Cauchy}$, $N = 500$, $T = 100$

Figure 3: Simulated randomization distribution for $\hat{\tau}^\dagger(1, 0; 1)$ under different choices of the parameter ϕ (defined in Example 1) and treatment probability $p(w)$. The rows index the parameter ϕ , which ranges over values $\{0.25, 0.5, 0.75\}$. The columns index the treatment probability $p(w)$, which ranges over values $\{0.25, 0.5, 0.75\}$. Panel (a) plots the simulated randomization distribution with normally distributed errors $\epsilon_{i,t} \sim N(0, 1)$ and $N = 100, T = 10$. Panel (b) plots the simulated randomization distribution with Cauchy distribution errors $\epsilon_{i,t} \sim \text{Cauchy}$ and $N = 500, T = 10$. Results are computed over 5,000 simulations.

causal effect. As we vary $\beta = \{-1, -0.9, \dots, 0.9, 1\}$, we also vary the parameter $\phi \in \{0.25, 0.5, 0.75\}$ and probability of treatment $p(w) \in \{0.25, 0.5, 0.75\}$ to investigate how rejection varies across a range of parameter values. We report the fraction of tests that reject the null hypothesis of zero average dynamic causal effects.

First, we investigate the rejection rate of the statistical test based on the normal asymptotic approximation for $H_0 : \bar{\tau}_t(1, 0; 0) = 0$ and $H_0 : \bar{\tau}_t^\dagger(1, 0; 1) = 0$. Figure 4 plots rejection rate curves against the null hypotheses as the parameter β varies for different choices of the parameter ϕ and treatment probability $p(w)$. The rejection rate against $H_0 : \bar{\tau}_t(1, 0; 0) = 0$ quickly converges to one as β moves away from zero across a range of simulations. This is encouraging as it indicates that the conservative variance bound still leads to informative tests. Unsurprisingly, when $\phi = 0.25$, the rejection rate against $H_0 : \bar{\tau}_t^\dagger(1, 0; 1) = 0$ is relatively low—lower values of ϕ imply less persistence in the causal effects across periods. When $\phi = 0.75$, there is substantial persistence in the causal effects across periods and we observe that the rejection rate curves look similar.

Next, we investigate the rejection rate of the statistical test based on the normal asymptotic

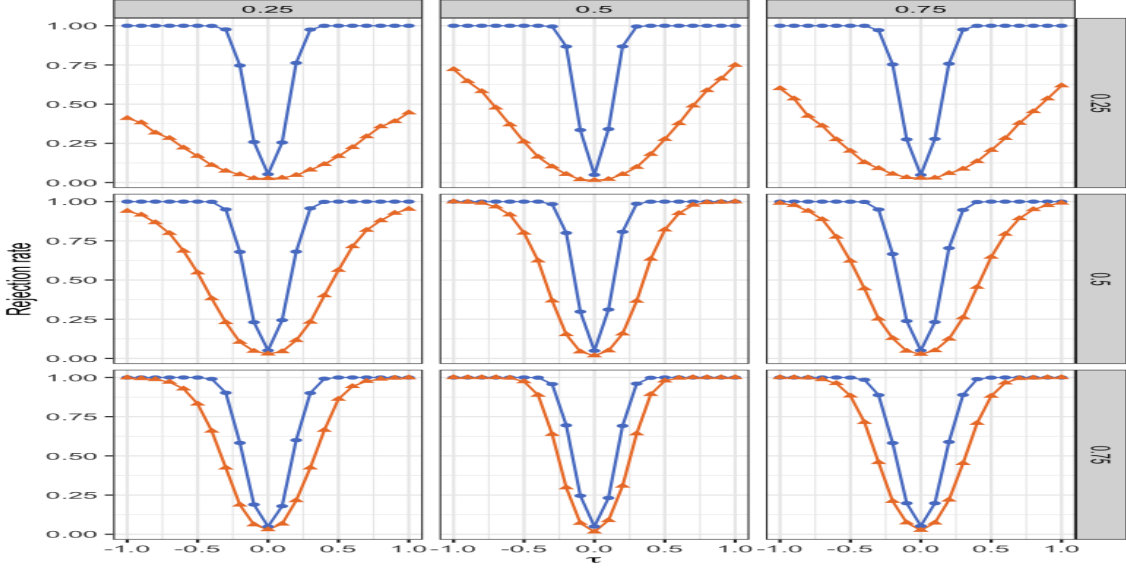


Figure 4: Rejection probabilities for a test of the null hypothesis $H_0 : \bar{\tau}_t(1, 0; 0) = 0$ and $H_0 : \bar{\tau}_t^\dagger(1, 0; 1) = 0$ as the parameter β varies under different choices of the parameter ϕ and treatment probability $p(w)$. The rejection rate curve against $H_0 : \bar{\tau}_t(1, 0; 0) = 0$ is plotted in blue and the rejection rate curve against $H_0 : \bar{\tau}_t^\dagger(1, 0; 1) = 0$ is plotted in orange. The rows index the parameter ϕ , which ranges over values $\{0.25, 0.5, 0.75\}$. The columns index the treatment probability $p(w)$, which ranges over values $\{0.25, 0.5, 0.75\}$. The simulations are conducted with normally distributed errors $\epsilon_{i,t} \sim N(0, 1)$ and $N = 1000$. Results are averaged over 5000 simulations.

approximation for $H_0 : \bar{\tau}_i^\dagger(1, 0; 0) = 0$ and $H_0 : \bar{\tau}_i^\dagger(1, 0; 1) = 0$, plotting the rejection rates in Figure 5. Once again, we observe that the rejection rate against $H_0 : \bar{\tau}_i^\dagger(1, 0; 0) = 0$ quickly converges to one as β moves away from zero across a range of simulations. Moreover, when the persistence of the causal effects is low ($\phi = 0.25$), the rejection rate against $H_0 : \bar{\tau}_i^\dagger(1, 0; 1) = 0$ is low.

Finally, we investigate the rejection rate of the statistical test based on the normal asymptotic approximation for $H_0 : \bar{\tau}^\dagger(1, 0; 1) = 0$ and $H_0 : \bar{\tau}^\dagger(1, 0; 1, 1) = 0$. Figure 6 plots rejection rate curves against the null hypotheses as the parameter β varies for different choices of the parameter ϕ and treatment probability $p(w)$. The qualitative patterns are similar as before.

6 Empirical application in experimental economics

We now apply our methods to reanalyze an experiment from Andreoni and Samuelson (2006) that tests a game-theoretic model of “rational cooperation” in a lab environment. Specifically, Andreoni and Samuelson (2006) studied how variations in the payoff structure of a two-player, twice-played prisoners’ dilemma affect the choices of players. The payoffs of the games were determined by two

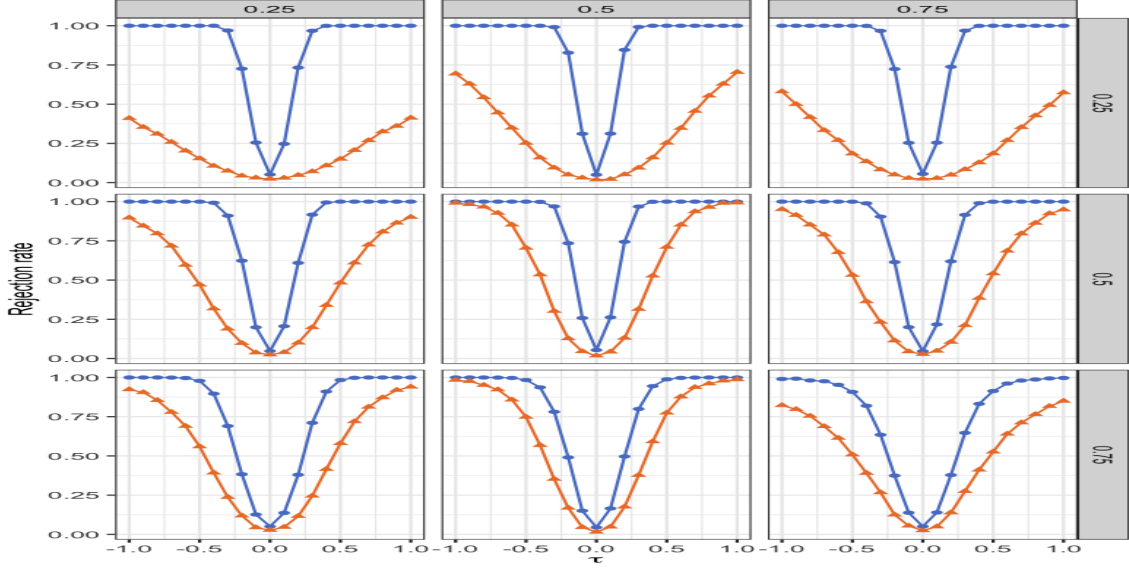


Figure 5: Rejection probabilities for a test of the null hypothesis $H_0 : \bar{\tau}_i^\dagger(1, 0; 0) = 0$ and $H_0 : \bar{\tau}_i^\dagger(1, 0; 1) = 0$ as the parameter β varies under different choices of the parameter ϕ and treatment probability $p(w)$. The rejection rate curve against $H_0 : \bar{\tau}_i^\dagger(1, 0; 0) = 0$ is plotted in blue and the rejection rate curve against $H_0 : \bar{\tau}_i^\dagger(1, 0; 1) = 0$ is plotted in orange. The rows index the parameter ϕ , which ranges over values $\{0.25, 0.5, 0.75\}$. The columns index the treatment probability $p(w)$, which ranges over values $\{0.25, 0.5, 0.75\}$. The simulations are conducted with normally distributed errors $\epsilon_{i,t} \sim N(0, 1)$ and $T = 1000$. Results are averaged over 5000 simulations.

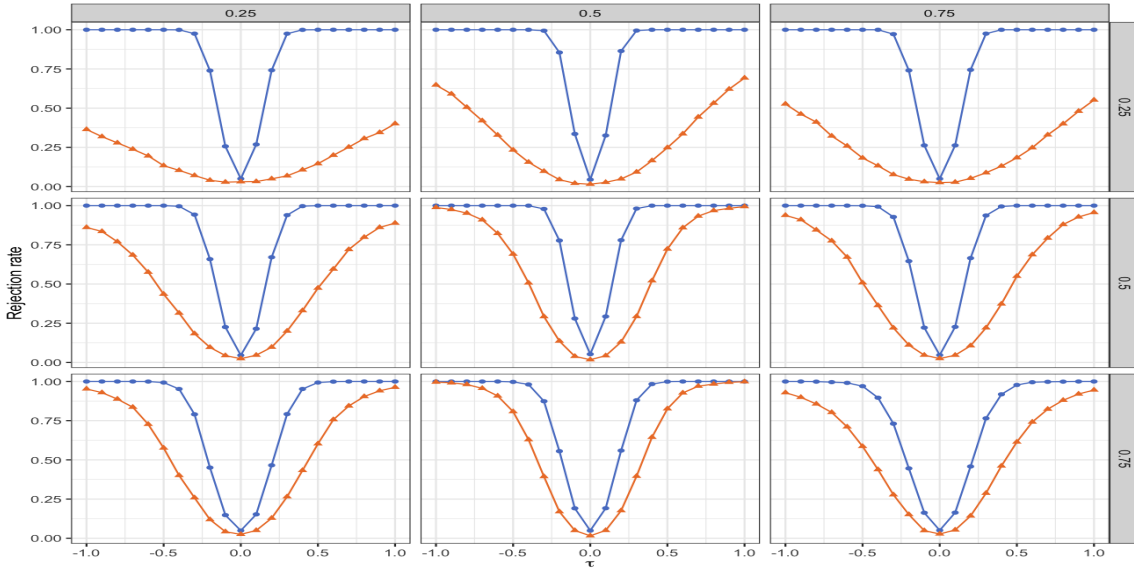


Figure 6: Rejection probabilities for a test of the null hypothesis $H_0 : \bar{\tau}_i^\dagger(1, 0; 0) = 0$ and $H_0 : \bar{\tau}_i^\dagger(1, 0; 1) = 0$ as the parameter β varies under different choices of the parameter ϕ and treatment probability $p(w)$. The rejection rate curve against $H_0 : \bar{\tau}_i^\dagger(1, 0; 0) = 0$ is plotted in blue and the rejection rate curve against $H_0 : \bar{\tau}_i^\dagger(1, 0; 1) = 0$ is plotted in orange. The rows index the parameter ϕ , which ranges over values $\{0.25, 0.5, 0.75\}$. The columns index the treatment probability $p(w)$, which ranges over values $\{0.25, 0.5, 0.75\}$. The simulations are conducted with normally distributed errors $\epsilon_{i,t} \sim N(0, 1)$ and $N = 100$, $T = 10$. Results are averaged over 5000 simulations.

	<i>C</i>	<i>D</i>		<i>C</i>	<i>D</i>
<i>C</i>	$(3x_1, 3x_1)$	$(0, 4x_1)$	<i>C</i>	$(3x_2, 3x_2)$	$(0, 4x_2)$
<i>D</i>	$(4x_1, 0)$	(x_1, x_1)	<i>D</i>	$(4x_2, 0)$	(x_2, x_2)
Period one			Period two		

Table 1: Stage games from twice-played prisoners’ dilemma in the experiment conducted by [Andreoni and Samuelson \(2006\)](#), where the parameters satisfy $x_1, x_2 \geq 0$, $x_1 + x_2 = 10$ and $\lambda = \frac{x_1}{x_1 + x_2}$. The choice *C* denotes “cooperate” and the choice *D* “defect.”

	Counts		
	0	1	Mean
Observed treatment, $W_{i,t}$	1136	1064	0.484
Observed outcome, $Y_{i,t}$	521	1679	0.763

Table 2: Summary statistics for the experiment in [Andreoni and Samuelson \(2006\)](#). The treatment $W_{i,t}$ equals one when the assigned value of λ is larger than 0.6. The outcome $Y_{i,t}$ equals one whenever the participant cooperates in period one of the twice-repeated prisoners’ dilemma. There are 110 participants and 1110 plays of the stage game in the experiment. Since each play of the stage game involves two participants, we observe 2220 choices total.

parameters $x_1, x_2 \geq 0$ such that $x_1 + x_2 = 10$. In each period, both players simultaneously select either *C* (cooperate) or *D* (defect) and subsequently received the payoffs associated with these choices. Table 1 summarizes the exact payoff structure; for example, if the players select (C, C) in period one, they receive $(3x_1, 3x_2)$, respectively. The game had two stages to allow the authors to estimate how changing the relative payoffs between period one and period two impacts the players’ behavior. Let $\lambda = \frac{x_2}{x_1 + x_2} \in [0, 1]$ govern the relative payoffs between the two periods of the prisoners’ dilemma; when $\lambda = 0$, all payoffs occurred in period one and when $\lambda = 1$, all payoffs occurred in period two. The authors predicted that when λ is large, players will cooperate more often in period one compared to when λ is small.

To investigate this hypothesis, [Andreoni and Samuelson \(2006\)](#) conducted a panel-based experiment to test this hypothesis. In one session of the experiment, 22 subjects were recruited to play 20 rounds of the twice-played prisoners’ dilemma in Table 1. In each round, participants were randomly matched into pairs, and each pair was then randomly assigned a value λ from the set $\{0, 0.1, \dots, 0.9, 1\}$ with equal probability. The authors conducted the experiment over five sessions for a total sample of 110 participants and 1110 plays of the stage game. Since each play of the stage game involves two participants, we observe the 2220 choices total.

The [Andreoni and Samuelson \(2006\)](#) experiment is a natural application for the methods we

developed in this paper for two reasons. First, since each subject plays the twice-played prisoners' dilemma many times under several randomly assigned payoff structures, the experiment has a typical panel structure. Second, the sequential nature of the games leaves open the possibility that past treatment assignments impact future actions; in other words, there may exist a dynamic causal effect that could bias standard methods for estimating causal effects from panel experiments.

In our notation, the outcome of interest Y is an indicator that equals one whenever the participant cooperated in the period one of the stage game, $N = 110$, and $T = 20$. The treatment W is binary and equals one whenever the assigned value λ is greater than 0.6, meaning that the payoffs are more concentrated in period two than period one of the stage game. For a given pair of subjects, the treatments are therefore always randomly assigned with probability $p = 5/11$. Table 2 summarizes the observed treatments and observed outcomes in the experiment.

One potential complication that may arise from the subjects playing against each other in the stage game is possible spillovers across units. The impact of such spillovers is, however, unlikely to be substantial as the matches are anonymous, and no players play each other more than once; we, therefore, ignore this concern in our analysis.¹¹ Finally, in Appendix C, we report additional results in which the outcome of interest Y is a player's total payoff in the stage game.

6.1 Analysis of unit and time-specific average dynamic causal effects

As detailed in Section 3, our nonparametric frameworks begin with estimating the unit-specific average dynamic causal effects. To illustrate the individual estimates, we focus on two randomly selected units in the experiment and construct estimates of their average i, t -th lag-0 dynamic causal effect, $\tau_{i,t}(1, 0; 0)$ (Definition 6). Figure 7 shows the nonparametric estimates $\hat{\tau}_{i,t}(1, 0; 0)$ for $t \in [T]$, for the two units. The figure also contains the nonparametric estimate of the average unit- i lag-0 dynamic causal effect $\hat{\tau}_{i,t}(1, 0; 0) = \frac{1}{T} \sum_{t=1}^T \hat{\tau}_{i,t}(1, 0; 0)$. The result shows that the point estimate of the average unit- i lag-0 dynamic causal effect is positive for both units, suggesting that a larger value of λ in the current game increases the likelihood of cooperation for both units. Since each unit only plays a total of twenty rounds, the estimated variance of these unit-specific estimators is quite large.

We next estimate period-specific, weighted average dynamic causal effects that pools information

¹¹Andreoni and Samuelson (2006) also ignore the possibility of spillovers across subjects in their analysis of the experiment.

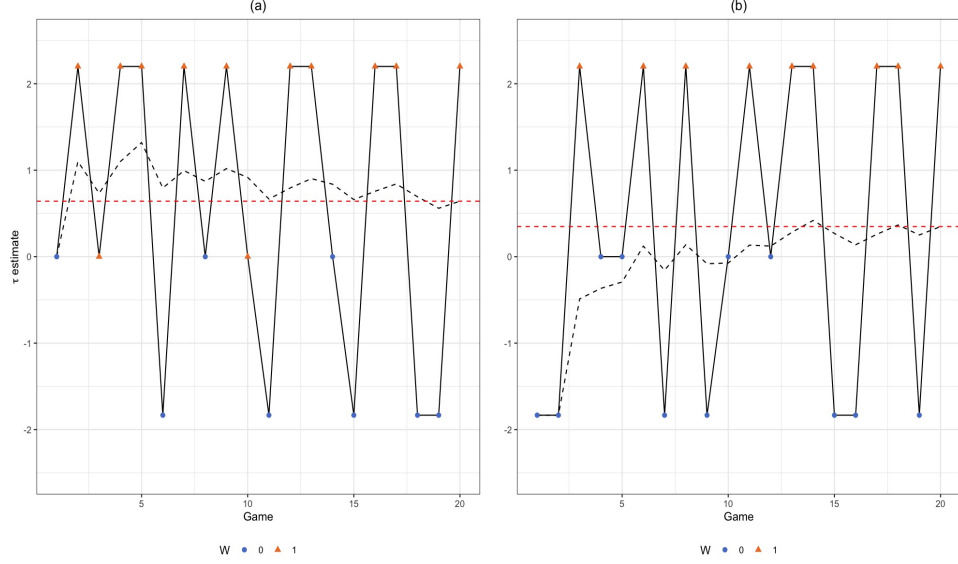


Figure 7: Estimates of the weighted average i, t -th lag-0 dynamic causal effect (Definition 6) of $W = 1\{\lambda \geq 0.6\}$ on cooperation in period one for two units in the experiment of Andreoni and Samuelson (2006). The solid black line plots the nonparametric estimator $\hat{\tau}_{i,t}(1, 0; 0)$ given in Remark 3.2. The dashed black line plots the running average of the period-specific estimator for each unit; that is, for each $t \in [T]$, $\frac{1}{t} \sum_{s=1}^t \hat{\tau}_{i,s}(1, 0; 0)$. The dashed red line plots the estimated weighted average unit- i lag-0 dynamic causal effect, $\hat{\tau}_i(1, 0; 0) = \frac{1}{T} \sum_{t=1}^T \hat{\tau}_{i,t}(1, 0; 0)$.

across units in order to gain precision. For each time period $t \in [T]$, we construct estimates based on the nonparametric estimator of the weighted average time- t , lag- p dynamic causal effect $\tau_t^\dagger(1, 0; p) = \frac{1}{N} \sum_{i=1}^N \tau_{i,t}^\dagger(1, 0; p)$ for $p = 0, 1, 2, 3$. For each value of p , the dashed black line in Figure 8 plots the estimates $\hat{\tau}_t^\dagger(1, 0; p)$ and the grey region plots a 95% pointwise conservative confidence band for the period-specific weighted average dynamic causal effects. Notice that across each value of p , there appears to be heterogeneity in the period-specific weighted causal dynamic causal effects across time periods. For example, for $p = 0$, the conservative confidence interval covers zero at $t = 5$ but it does not cover zero at $t = 15$. Moreover, aside from two periods, all point estimates for the period-specific lag-0 weighted average dynamic causal effects are positive. In contrast, there are many positive and negative point estimates for period-specific weighted average dynamic causal effects with $p \geq 1$. This suggests that the treatment $W = 1\{\lambda \geq 0.6\}$ may have contemporaneous causal effects on cooperation in period one of the stage game and that it may not have dynamic causal effects.

To further investigate this, the solid blue line in Figure 8 plots the nonparametric estimator the total lag- p weighted average causal effect $\tau^\dagger(1, 0; p)$ for $p = 0, 1, 2, 3$, which further pools information across all units and time periods. The dashed blue lines plot the conservative confidence interval

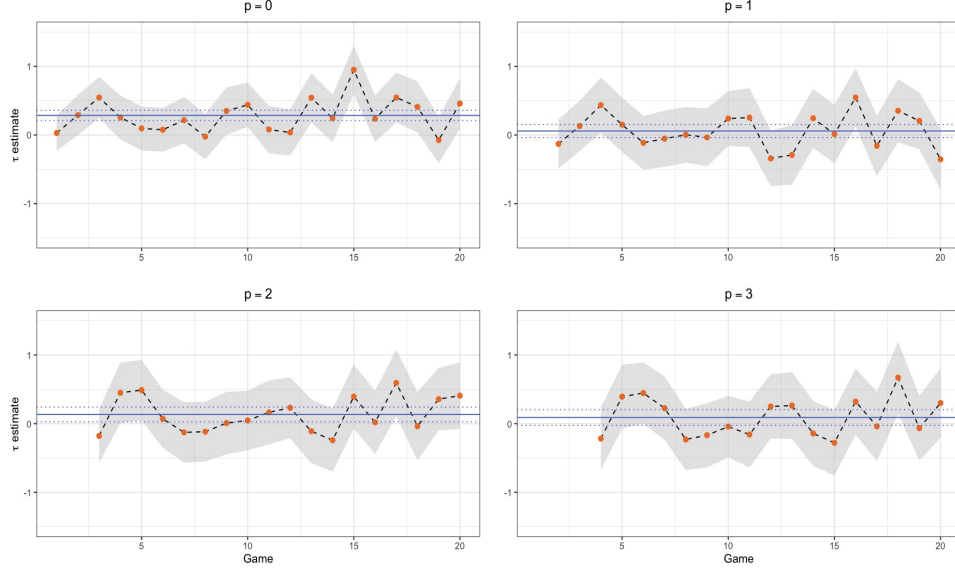


Figure 8: Estimates of the time- t lag- p weighted average dynamic causal effect, $\tau_t^\dagger(1, 0; p)$ of $W = 1\{\lambda \geq 0.6\}$ on cooperation in period one based on the experiment of [Andreoni and Samuelson \(2006\)](#) for each time period $t \in [T]$ and $p = 0, 1, 2, 3$. The black dashed line plots the nonparametric estimator of the time- t lag- p weighted average dynamic causal effect, $\hat{\tau}_t^\dagger(1, 0; p)$, for each period $t \in [T]$. The grey region plots the 95% point-wise confidence band for $\tau_t^\dagger(1, 0; p)$ based on the conservative estimator of the asymptotic variance of the nonparametric estimator (Theorem 3.2). The solid blue line plots the nonparametric estimator of the total lag- p weighted average dynamic causal effect, $\hat{\tau}^\dagger(1, 0; p)$ and the dashed blue lines plot the 95% confidence interval for $\tau^\dagger(1, 0; p)$ based on the conservative estimator of the asymptotic variance of the nonparametric estimator.

for the total lag- p weighted average causal effect. As can be seen, the weak null hypothesis that $\tau(1, 0; 0) = 0$ can be soundly rejected, indicating that the treatment has a positive contemporaneous effect on cooperation in period one of the stage game and confirming the hypothesis of [Andreoni and Samuelson \(2006\)](#). However, the results are less stark for dynamic causal effects. For $p = 1, 3$, zero is covered by the conservative confidence interval but not for $p = 2$. Table 3 summarizes these estimates of the total lag- p weighted average causal effects.

	lag- p			
	0	1	2	3
Point estimate, $\hat{\tau}^\dagger(1, 0; p)$	0.285	0.058	0.134	0.089
Conservative p-value	0.000	0.226	0.013	0.126
Randomization p-value	0.000	0.263	0.012	0.114

Table 3: Estimates of the total lag- p weighted average dynamic causal effect for $p = 0, 1, 2, 3$. The conservative p-value reports the p-value associated with testing the weak null hypothesis of no average dynamic causal effects, $H_0 : \tau^\dagger(1, 0; p) = 0$, using the conservative estimator of the asymptotic variance of the nonparametric estimator (Theorem 3.2). The randomization p-value reports the p-value associated with randomization test of the sharp null of dynamic causal effects, $H_0 : \tau_{i,t}(w, \tilde{w}; p) = 0$ for all $i \in [N], t \in [T]$. The randomization p-values are constructed based on 10,000 draws.

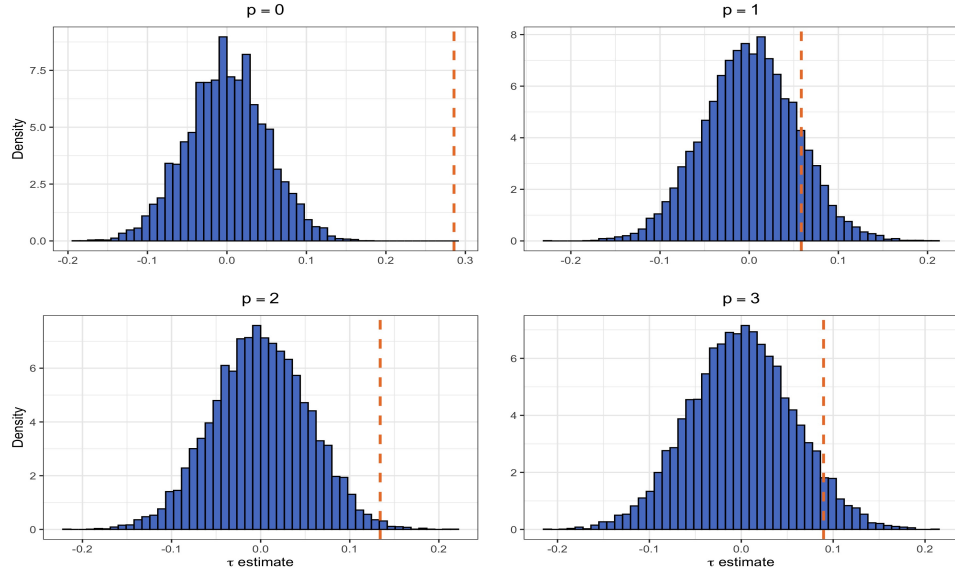


Figure 9: Estimated randomization distribution of the nonparametric estimator of the total lag- p weighted average dynamic causal effect, $\hat{\tau}^\dagger(1, 0; p)$, under the sharp null of no dynamic causal effect, $\tau_{i,t}(w, w; p) = 0$ for all $i \in [N], t \in [T]$. The dashed orange line plots the estimate, $\hat{\tau}^\dagger(1, 0; p)$ at the realized treatments in the experiment of [Andreoni and Samuelson \(2006\)](#). The estimated randomization distributions are constructed based on 10,000 draws.

6.2 Exact randomization inference on total average dynamic causal effects

We further unpack these results using randomization tests based on the sharp null of no dynamic causal effects. We construct the randomization distribution for the nonparametric estimator of the total lag- p weighted average dynamic causal effect $\hat{\tau}^\dagger(1, 0; p)$ for $p = 0, 1, 2, 3$ under the sharp null hypothesis of no lag- p dynamic dynamical causal effects for all units and time periods; $H_0 : \tau_{i,t}(w, \tilde{w}; p) = 0$ for all $i \in [N], t \in [T]$. Under this sharp null hypothesis, all relevant potential outcomes are known and we can construct the randomization distribution by redrawing the entire treatment panel according to the known treatment assignment mechanism. When redrawing treatment paths, we do so in a manner that respects the realized pairs of subjects in the experiment, meaning that subjects that are paired in the same round receive the same treatment.

Figure 9 plots the randomization distributions for $p = 0, 1, 2, 3$ along with the point estimate $\hat{\tau}^\dagger(1, 0; p)$ at the realized treatment panel. The randomization distributions appear to be smooth and symmetric around zero. The p-value for the randomization test at $p = 0$ is approximately zero, strongly rejected the sharp null of no contemporaneous dynamic causal effects for all units. This further confirms the hypothesis of [Andreoni and Samuelson \(2006\)](#) that higher values of λ induce

more cooperation in the twice-repeated prisoners’ dilemma. There is some suggestive evidence of dynamic causal effects. While we are unable to reject the sharp null of no dynamic causal effects at lags $p = 1, 3$, we are able to reject at the 5% level for $p = 2$ (p-value equals 0.012). This suggests that there may have been dynamic causal effects of the treatment on cooperative behavior across rounds of the twice-repeated prisoners’ dilemma. Table 3 summarizes randomization p-values for the total lag- p weighted average causal effects.

7 Conclusion

In this paper, we developed a potential outcome model for studying dynamic causal effects in a panel experiment. Crucially, our analysis provided the first formal framework for incorporating design-based uncertainty in panel experiments—meaning that we treated the potential outcome as fixed, and the only source of randomization comes from the treatment assignments. We defined new panel-based dynamic causal estimands such as the lag- p dynamic causal effect and introduced an associated nonparametric estimator. We showed that this estimator is unbiased for lag- p dynamic causal effects over the randomization distribution, and we derived its finite population asymptotic distribution. We then developed tools to conduct inference on these dynamic causal effects—introducing both an asymptotically conservative test for Neyman-type weak nulls and a randomization-based test for Fisher-type sharp nulls. We also derived the finite population probability limit of the linear unit fixed effects estimator and two-way fixed effects estimator, showing that these estimators are asymptotically biased in the presence of dynamic causal effects. Finally, we illustrated our results in an extensive simulation study, and we reanalyzed an experiment conducted by [Andreoni and Samuelson \(2006\)](#).

References

Abadie, A., S. C. Athey, G. W. Imbens, and J. Wooldridge (2017). When should you adjust standard errors for clustering? Technical report.

Abadie, A., S. C. Athey, G. W. Imbens, and J. Wooldridge (2020). Sampling-based vs. design-based uncertainty in regression analysis. Technical Report 1.

Abraham, S. and L. Sun (2019). Estimating dynamic treatment effects in event studies with heterogeneous treatment effects. Technical report.

Allegretto, S., A. Dube, M. Reich, and B. Zipperer (2017). Credible research designs for minimum wage studies: A response to neumark, salas, and wascher. *ILR Review* 70(3), 559–592.

Anderson, T. and C. Hsiao (1982). Formulation and estimation of dynamic models using panel data. *Journal of Econometrics* 18, 47–82.

Andreoni, J. and L. Samuelson (2006). Building rational cooperation. *Journal of Economic Theory* 127, 117–154.

Arellano, M. (2003). *Panel Data Econometrics*. Oxford: Oxford University Press.

Arellano, M., R. Blundell, and S. Bonhomme (2017). Earnings and consumption dynamics: A nonlinear panel data framework. 85, 693–734.

Arellano, M. and S. R. Bond (1991). Some tests of specification for panel data: Monte Carlo evidence and an application to employment equations. *Review of Economic Studies* 58, 277–297.

Arellano, M. and S. Bonhomme (2012). Nonlinear panel data analysis. *Annual Review of Economics* 3, 395–424.

Arkhangelsky, D. and G. Imbens (2019). Double-robust identification for causal panel data models. Technical report, arXiv preprint arXiv:1909.09412.

Athey, S., M. Bayati, N. Doudchenko, G. Imbens, and K. Koshravi (2018). Matrix completion methods for causal panel data models. Technical report, arXiv preprint arXiv 1710.10251.

Athey, S. and G. Imbens (2018). Design-based analysis in difference-in-differences settings with staggered adoption. Technical report, arXiv preprint arXiv:1808.05293.

Bellemare, C., L. Bissonnette, and S. Kroger (2014). Statistical power of within and between-subjects designs in economic experiments. Technical report, IZA Working Paper No. 8583.

Bellemare, C., L. Bissonnette, and S. Kroger (2016). Simulating power of economic experiments: the powerbbk package. *Journal of the Economic Science Association* 2, 157–168.

Ben-Porath, Y. (1967). The Production of Human Capital and the Life Cycle of Earnings. *Journal of Political Economy* 75, 352–365.

Bojinov, I. and N. Shephard (2019). Time series experiments and causal estimands: exact randomization tests and trading. *Journal of the American Statistical Association*. Forthcoming.

Boruvka, A., D. Almirall, K. Witkiwitz, and S. A. Murphy (2018). Assessing time-varying causal effect moderation in mobile health. *Journal of the American Statistical Association* 113, 1112–1121.

Boryusak, K. and X. Jaravel (2017). Revisiting event study designs, with an application to the estimation of the marginal propensity to consume. Technical report.

Browning, M., M. Ejrnaes, and J. Alvarez (2010). Modelling income processes with lots of heterogeneity. *Review of Economic Studies* 77, 1353–1381.

Charness, G., U. Gneezy, and M. A. Kuhn (2012). Experimental methods: Between-subject and within-subject design. *Journal of Economic and Business Organization* 81(1), 1–8.

Cox, D. R. (1958). *Planning of Experiments*. Oxford: Wiley.

Cunha, F., J. J. Heckman, L. Lochner, and D. V. Masterov (2006, January). Chapter 12 Interpreting the Evidence on Life Cycle Skill Formation. In E. Hanushek and F. Welch (Eds.), *Handbook of the Economics of Education*, Volume 1, pp. 697–812. Elsevier.

Cunha, F., J. J. Heckman, and S. M. Schennach (2010). Estimating the Technology of Cognitive and Noncognitive Skill Formation. *Econometrica* 78(3), 883–931.

Czibor, E., D. Jimenez-Gomez, and J. A. List (2019). The dozen things experimental economists should do (more of). *Southern Economic Journal* 86(2), 371–432.

de Chaisemartin, C. and X. D'Haultfoeuille (2019). Two-way fixed effects estimators with heterogeneous treatment effects. Unpublished paper: University of California at Santa Barbara.

Ding, P. (2017). A paradox from randomization-based causal inference. *Statistical Science* 32, 331–345.

Freedman, D. A. (2008). On regression adjustments to experimental data. *Advances in Applied Mathematics* 40(2), 180–193.

Griliches, Z. (1977). Estimating the Returns to Schooling: Some Econometric Problems. *Econometrica* 45, 1–22.

Hall, P. and C. C. Heyde (1980). *Martingale Limit Theory and its Applications*. San Diego, California, USA: Academic Press.

Han, S. (2019). Identification in nonparametric models for dynamic treatment effects. Unpublished paper: Department of Economics, University of Texas, Austin.

Hernan, M. A. and J. M. Robins (2019). *Causal Inference*. Boca Raton, Florida, USA: Chapman & Hall. Forthcoming.

Holland, P. W. (1986). Statistics and causal inference. *Journal of the American Statistical Association* 81, 945–960.

Horvitz, D. G. and D. J. Thompson (1952). A generalization of sampling without replacement from a finite universe. *Journal of the American Statistical Association* 47, 663–685.

Hull, P. (2018). Estimating treatment effects in mover designs. Unpublished paper: University of Chicago.

Imai, K. and I. Kim (2019a). On the use of two-way fixed effects regression models for causal inference with panel data. Unpublished paper: Harvard University.

Imai, K. and I. Kim (2019b). When should we use unit fixed effects regression models for causal inference with longitudinal data? *American Journal of Political Science* 63, 467–490.

Imbens, G. W. and D. B. Rubin (2015). *Causal Inference for Statistics, Social and Biomedical Sciences: An Introduction*. Cambridge, United Kingdom: Cambridge University Press.

Kempthorne, O. (1955). The randomization theory of experimental inference. *Journal of the American Statistical Association* 50, 946–967.

Lechner, M. (2011). The estimation of causal effects by difference-in-difference methods. *Foundations and Trends in Econometrics* 4, 165–224.

Li, X. and P. Ding (2017). General forms of finite population central limit theorems with applications to causal inference. *Journal of the American Statistical Association* 112(520), 1759–1769.

Lillie, E. O., B. Patay, J. Diamant, B. Issell, E. J. Topol, and N. J. Schork (2011). The n-of-1 clinical trial: the ultimate strategy for individualizing medicine? *Personalized medicine* 8(2), 161–173.

Murphy, S. A., M. J. van der Laan, J. M. Robins, and C. P. P. R. Group (2001). Marginal mean models for dynamic regimes. *Journal of the American Statistical Association* 96, 1410–1423.

Nerlove, M. (1971). Further evidence on the estimation of dynamic economic relations from a time series of cross-sections. *Econometrica* 39, 359–387.

Neyman, J. (1923). On the application of probability theory to agricultural experiments. Essay on principles. Section 9. *Statistical Science* 5, 465–472. Originally published 1923, republished in 1990, translated by Dorota M. Dabrowska and Terence P. Speed.

Nickell, S. J. (1981). Biases in dynamic models with fixed effects. *Econometrica* 49, 1417–1426.

Pearl, J. and D. Mackenzie (2018). *The Book of Why: The New Science of Cause and Effect*. Basic Books.

Rambachan, A. and N. Shephard (2019). A nonparametric causal model for macroeconomics: from potential outcome time series to local projection and impulse response functions. Unpublished paper: Department of Economics, Harvard University.

Robins, J. M. (1986). A new approach to causal inference in mortality studies with sustained exposure periods: Application to control of the healthy worker survivor effect. *Mathematical Modelling* 7, 1393–1512.

Robins, J. M. (1994). Correcting for non-compliance in randomization trials using structural nested mean models. *Communications in Statistics — Theory and Methods* 23, 2379–2412.

Rubin, D. B. (1974). Estimating causal effects of treatments in randomized and nonrandomized studies. *Journal of Educational Psychology* 66, 688–701.

Rubin, D. B. (1980). Randomization analysis of experimental data: The Fisher randomization test comment. *Journal of the American Statistical Association* 75, 591–593.

Sobel, M. E. (2006). What do randomized studies of housing mobility demonstrate? causal inference in the face of interference. *Journal of the American Statistical Association* 101, 1398–1407.

Panel-Based Experiments and Dynamic Causal Effects: A finite population Perspective

Online Appendix

Iavor Bojinov Ashesh Rambachan Neil Shephard

A Proofs of Main Results

Proof of Theorem 3.1

We begin the proof with a Lemma that will be used later on.

Lemma A.1. *Assume a potential outcome panel obeys Assumption 6. Define, for any $\mathbf{w} \in \mathcal{W}^{(p+1)}$, the random function $Z_{i,t-p:t}(\mathbf{w}) := p_{i,t-p}(\mathbf{w})^{-1} \mathbb{1}\{W_{i,t-p:t} = \mathbf{w}\}$. Then, over the randomization mechanism, $\mathbb{E}(Z_{i,t-p:t}(\mathbf{w})|\mathcal{F}_{i,t-p-1}) = 1$ and $\text{Var}(Z_{i,t-p:t}(\mathbf{w})|\mathcal{F}_{i,t-p-1}) = p_{i,t-p}(\mathbf{w})^{-1}(1 - p_{i,t-p}(\mathbf{w}))$, and $\text{Cov}(Z_{i,t-p:t}(\mathbf{w}), Z_{i,t-p:t}(\tilde{\mathbf{w}})|\mathcal{F}_{i,t-p-1}) = -1$ for all $\mathbf{w} \neq \tilde{\mathbf{w}}$. Under non-interference, $Z_{i,t-p:t}(\mathbf{w})$ and $Z_{j,t-p:t}(\mathbf{w})$ are, conditioning on $\mathcal{F}_{1:N,t-p-1}$, independent for $i \neq j$.*

Proof. The expectation is by construction, the variance comes from the variance of a Bernoulli trial. The conditional independence is by the non-interference assumption. \square

For any $\mathbf{w}, \tilde{\mathbf{w}} \in \mathcal{W}^{(p+1)}$, let $u_{i,t-p}(\mathbf{w}, \tilde{\mathbf{w}}; p) = \hat{\tau}_{i,t}(\mathbf{w}, \tilde{\mathbf{w}}; p) - \tau_{i,t}(\mathbf{w}, \tilde{\mathbf{w}}; p)$ be the estimation error. Now

$$u_{i,t-p}(\mathbf{w}, \tilde{\mathbf{w}}; p) = Y_{i,t}(w_{i,1:t-p-1}^{obs}, \mathbf{w})(Z_{i,t-p:t}(\mathbf{w}) - 1) - Y_{i,t}(w_{i,1:t-p-1}^{obs}, \tilde{\mathbf{w}})(Z_{i,t-p:t}(\tilde{\mathbf{w}}) - 1).$$

Hence the zero condition expectation follows using Lemma A.1. Then,

$$\begin{aligned} \text{Var}(u_{i,t-p}(\mathbf{w}, \tilde{\mathbf{w}}; p)|\mathcal{F}_{i,t-p-1}) &= Y_{i,t}(w_{i,1:t-p-1}^{obs}, \mathbf{w})^2 \text{Var}(Z_{i,t-p:t}(\mathbf{w})|\mathcal{F}_{i,t-p-1}) \\ &+ Y_{i,t}(w_{i,1:t-p-1}^{obs}, \tilde{\mathbf{w}})^2 \text{Var}(Z_{i,t-p:t}(\tilde{\mathbf{w}})|\mathcal{F}_{i,t-p-1}) \\ &- 2Y_{i,t}(w_{i,1:t-p-1}^{obs}, \mathbf{w})Y_{i,t}(w_{i,1:t-p-1}^{obs}, \tilde{\mathbf{w}}) \text{Cov}(Z_{i,t-p:t}(\mathbf{w}), Z_{i,t-p:t}(\tilde{\mathbf{w}})|\mathcal{F}_{i,t-p-1}) \\ &= Y_{i,t}(w_{i,1:t-p-1}^{obs}, \mathbf{w})^2 p_{i,t-p}(\mathbf{w})^{-1}(1 - p_{i,t-p}(\mathbf{w})) \\ &+ Y_{i,t}(w_{i,1:t-p-1}^{obs}, \tilde{\mathbf{w}})^2 p_{i,t-p}(\tilde{\mathbf{w}})^{-1}(1 - p_{i,t-p}(\tilde{\mathbf{w}})) \\ &- 2Y_{i,t}(w_{i,1:t-p-1}^{obs}, \mathbf{w})Y_{i,t}(w_{i,1:t-p-1}^{obs}, \tilde{\mathbf{w}}). \end{aligned}$$

Simplifying gives the result on the variance of the estimation error. Then,

$$\begin{aligned} &\text{Cov}(u_{i,t-p}(\mathbf{w}, \tilde{\mathbf{w}}; p), u_{i,t-p}(\bar{\mathbf{w}}, \hat{\mathbf{w}}; p)|\mathcal{F}_{i,t-p-1}) \\ &= Y_{i,t}(w_{i,1:t-p-1}^{obs}, \mathbf{w})Y_{i,t}(w_{i,1:t-p-1}^{obs}, \bar{\mathbf{w}}) \text{Cov}(Z_{i,t-p:t}(\mathbf{w}), Z_{i,t-p:t}(\bar{\mathbf{w}})|\mathcal{F}_{i,t-p-1}) \\ &- Y_{i,t}(w_{i,1:t-p-1}^{obs}, \mathbf{w})Y_{i,t}(w_{i,1:t-p-1}^{obs}, \hat{\mathbf{w}}) \text{Cov}(Z_{i,t-p:t}(\mathbf{w}), Z_{i,t-p:t}(\hat{\mathbf{w}})|\mathcal{F}_{i,t-p-1}) \\ &- Y_{i,t}(w_{i,1:t-p-1}^{obs}, \tilde{\mathbf{w}})Y_{i,t}(w_{i,1:t-p-1}^{obs}, \bar{\mathbf{w}}) \text{Cov}(Z_{i,t-p:t}(\tilde{\mathbf{w}}), Z_{i,t-p:t}(\bar{\mathbf{w}})|\mathcal{F}_{i,t-p-1}) \\ &Y_{i,t}(w_{i,1:t-p-1}^{obs}, \tilde{\mathbf{w}})Y_{i,t}(w_{i,1:t-p-1}^{obs}, \hat{\mathbf{w}}) \text{Cov}(Z_{i,t-p:t}(\tilde{\mathbf{w}}), Z_{i,t-p:t}(\hat{\mathbf{w}})|\mathcal{F}_{i,t-p-1}) \\ &= -Y_{i,t}(w_{i,1:t-p-1}^{obs}, \mathbf{w})Y_{i,t}(w_{i,1:t-p-1}^{obs}, \bar{\mathbf{w}}) + Y_{i,t}(w_{i,1:t-p-1}^{obs}, \mathbf{w})Y_{i,t}(w_{i,1:t-p-1}^{obs}, \hat{\mathbf{w}}) \\ &+ Y_{i,t}(w_{i,1:t-p-1}^{obs}, \tilde{\mathbf{w}})Y_{i,t}(w_{i,1:t-p-1}^{obs}, \bar{\mathbf{w}}) - Y_{i,t}(w_{i,1:t-p-1}^{obs}, \tilde{\mathbf{w}})Y_{i,t}(w_{i,1:t-p-1}^{obs}, \hat{\mathbf{w}}) \end{aligned}$$

Finally, conditional independence of the errors follows due to non-interference of the treatments. \square

Proof of Theorem 3.2

Only the third results requires a new proof. In particular, the first result is a reinterpretation of the classic cross-sectional result using a triangular array central limit theorem, for the usual Lindeberg condition must hold due to the bounded potential outcomes and the treatments being probabilistic. The second result follows from results in [Bojinov and Shephard \(2019\)](#), who use a martingale difference array central limit theorem.

The third result, which holds for NT going to infinity, can be split into three parts. For NT to go to infinity we must have either: (i) T goes to infinity with N finite, (ii) N goes to infinity with T finite, or (iii) both N and T go to infinity. In the case (i), we apply the martingale difference CLT but now where each time period we have preaveraged the cross-sectional errors over the N terms. The preaverage is still a martingale difference, so the technology is the same. In the case (ii) we preaverage the time aspect. Then we are back to a standard triangular array CLT. As we have both (i) and (ii), then (iii) must hold. \square

Proof of Proposition 4.1

Under linear potential outcomes,

$$Y_{i,t}(W_{i,1:t}) - Y_{i,t}(\tilde{w}_{i,1:t}) = \sum_{s=0}^{t-1} \beta_{i,t,s}(W_{i,t-s} - \tilde{w}_{i,t-s}).$$

Focus on the counterfactual $\tilde{w}_{i,1:t} = \mathbf{0}$, then

$$Y_{i,t} = Y_{i,t}(W_{i,1:t}) = \bar{Y}_t(\mathbf{0}) + \sum_{s=0}^{t-1} \beta_{i,t,s} W_{i,t-s} + \dot{\nu}_{i,t}(\mathbf{0}), \quad \dot{\nu}_{i,t}(\mathbf{0}) = Y_{i,t}(\mathbf{0}) - \bar{Y}_t(\mathbf{0}), \quad \bar{Y}_t(\mathbf{0}) = \frac{1}{N} \sum_{i=1}^N Y_{i,t}(\mathbf{0}).$$

Of course,

$$\dot{Y}_{i,t} = Y_{i,t} - \bar{Y}_t = \sum_{s=0}^{t-1} \{\beta_{i,t,s} W_{i,t-s} - \frac{1}{N} \sum_{j=1}^N \beta_{j,t,s} W_{j,t-s}\} + \dot{\nu}_{i,t}(\mathbf{0}).$$

Under homogeneity,

$$\dot{Y}_{i,t} = \sum_{s=0}^{t-1} \{\beta_{t,s} (W_{i,t-s} - \frac{1}{N} \sum_{j=1}^N W_{j,t-s})\} + \dot{\nu}_{i,t}(\mathbf{0}).$$

Stacking everything, this becomes

$$\dot{Y}_t = \dot{W}_t \beta_t + \dot{\nu}_t(\mathbf{0}),$$

so

$$\hat{\beta}_t = (\dot{W}_t' \dot{W}_t)^{-1} \dot{W}_t' \dot{Y}_t = \beta_t + (\dot{W}_t' \dot{W}_t)^{-1} \dot{W}_t' \dot{\nu}_t(\mathbf{0}).$$

The important unusual point here is that $\dot{\nu}_t(\mathbf{0})$ is non-stochastic and that \dot{W}_t is random, exactly the opposite of the case often discussed in the statistical analysis of linear regression. Now

$$\frac{1}{N} \dot{W}_t' \dot{W}_t = \frac{1}{N} \sum_{i=1}^N \dot{W}_{i,t} \dot{W}_{i,t}',$$

and

$$\frac{1}{N} \dot{W}'_t \dot{\nu}_t(\mathbf{0}) = \frac{1}{N} \sum_{i=1}^N \dot{W}_{i,t} \dot{\nu}_{i,t}(\mathbf{0}) = \frac{1}{N} \sum_{i=1}^N (\dot{W}_{i,t} - \dot{\mu}_{i,t,N}) \dot{\nu}_{i,t}(\mathbf{0}) + \frac{1}{N}$$

Then, under non-interference of Assumption 5,

$$\frac{1}{N} \sum_{i=1}^N \dot{W}_{i,t} \dot{W}'_{i,t} | \mathcal{F}_{1:N,0,T} \xrightarrow{p} \Gamma_{2,t},$$

recalling $\dot{\nu}_{i,t}(\mathbf{0})$ is non-stochastic and applying Assumptions 4(b) and 4(c), then Slutsky's theorem delivers the result stated in the paper. \square

Proof of Proposition 4.2

Begin by writing the observed outcomes as

$$Y_{i,t} = Y_{i,t}(\mathbf{0}) + \sum_{s=1}^t \beta_{i,t,t-s} W_{i,s}.$$

Similarly, write $\bar{Y}_i = \bar{Y}_i(\mathbf{0}) + \bar{\beta} \bar{W}_i$, where $\bar{\beta} \bar{W}_i = \frac{1}{T} \sum_{t=1}^T \sum_{s=1}^t \beta_{i,t,t-s} W_{i,s}$. The transformed outcome can be then written as

$$\check{Y}_{i,t} = \sum_{s=1}^t \beta_{i,t,t-s} W_{i,s} - \bar{\beta} \bar{W}_i + \check{\nu}_{i,t}(\mathbf{0}).$$

Consider the numerator of the unit fixed effects estimator. Substituting in, we arrive at

$$\begin{aligned} \frac{1}{NT} \sum_{i=1}^N \sum_{t=1}^T \check{Y}_{i,t} \check{W}_{i,t} &= \frac{1}{NT} \sum_{i=1}^N \sum_{t=1}^T \beta_{i,t,0} W_{i,t} \check{W}_{i,t} + \frac{1}{NT} \sum_{i=1}^N \sum_{t=1}^T \left(\sum_{s=1}^{t-1} \beta_{i,t,t-s} W_{i,s} \check{W}_{i,t} \right) + \frac{1}{NT} \sum_{i=1}^N \sum_{t=1}^T \check{\nu}_{i,t}(\mathbf{0}) \check{W}_{i,t} \\ &= \frac{1}{T} \sum_{t=1}^T \left(\frac{1}{N} \sum_{i=1}^N \beta_{i,t,0} W_{i,t} \check{W}_{i,t} \right) + \frac{1}{T} \sum_{t=1}^T \sum_{s=1}^{t-1} \left(\frac{1}{N} \sum_{i=1}^N \beta_{i,t,t-s} W_{i,s} \check{W}_{i,t} \right) + \frac{1}{T} \sum_{t=1}^T \left(\frac{1}{N} \sum_{i=1}^N \check{\nu}_{i,t}(\mathbf{0}) \check{W}_{i,t} \right). \end{aligned}$$

Therefore, for fixed T as $N \rightarrow \infty$,

$$\begin{aligned} \frac{1}{T} \sum_{t=1}^T \left(\frac{1}{N} \sum_{i=1}^N \beta_{i,t,0} W_{i,t} \check{W}_{i,t} \right) &\xrightarrow{p} \frac{1}{T} \sum_{t=1}^T \check{\kappa}_{W,\beta,t,t}, \\ \frac{1}{T} \sum_{t=1}^T \sum_{s=1}^{t-1} \left(\frac{1}{N} \sum_{i=1}^N \beta_{i,t,t-s} W_{i,s} \check{W}_{i,t} \right) &\xrightarrow{p} \frac{1}{T} \sum_{t=1}^T \sum_{s=1}^{t-1} \check{\kappa}_{W,\beta,t,s}, \\ \frac{1}{T} \sum_{t=1}^T \left(\frac{1}{N} \sum_{i=1}^N \check{\nu}_{i,t}(\mathbf{0}) \check{W}_{i,t} \right) &= \frac{1}{T} \sum_{t=1}^T \check{\delta}_t. \end{aligned}$$

Similarly, the denominator converges to

$$\frac{1}{NT} \sum_{t=1}^T \sum_{i=1}^N \check{W}_{i,t}^2 \xrightarrow{p} \frac{1}{T} \sum_{t=1}^T \check{\sigma}_{W,t}^2.$$

The result then follows by Slutsky. \square

Proof of Proposition 4.3

Begin by writing

$$Y_{i,t} = Y_{i,t}(\mathbf{0}) + \sum_{s=1}^t \beta_{i,t,s} W_{i,s}.$$

Then, $\bar{Y}_t = \bar{Y}_t(\mathbf{0}) + \bar{\beta} \bar{W}_t$, $\bar{Y}_i = \bar{Y}_i(\mathbf{0}) + \bar{\beta} \bar{W}_i$ and $\bar{Y} = \bar{Y}(\mathbf{0}) + \bar{\beta} \bar{W}$. Therefore,

$$\dot{\bar{Y}}_{i,t} = \dot{\bar{Y}}_{i,t}(\mathbf{0}) + \left(\sum_{s=1}^t \beta_{i,t,s} W_{i,s} - \bar{\beta} \bar{W} \right) - (\bar{\beta} \bar{W}_t - \bar{\beta} \bar{W}) - (\bar{\beta} \bar{W}_i - \bar{\beta} \bar{W}).$$

Define the error $\varepsilon_{i,t,N,T}(\mathbf{0}) = \dot{\bar{Y}}_{i,t}(\mathbf{0})$. Consider the numerator of the unit fixed effects estimator. Substituting in,

$$\begin{aligned} \frac{1}{NT} \sum_{i=1}^N \sum_{t=1}^T \dot{\bar{Y}}_{i,t} \dot{\bar{W}}_{i,t} &= \frac{1}{NT} \sum_{i=1}^N \sum_{t=1}^T \beta_{i,t,0} W_{i,t} \dot{\bar{W}}_{i,t} + \frac{1}{NT} \sum_{i=1}^N \sum_{t=1}^T \sum_{s=1}^{t-1} \beta_{i,t,s} W_{i,s} \dot{\bar{W}}_{i,t} + \frac{1}{NT} \sum_{i=1}^N \sum_{t=1}^T \varepsilon_{i,t,N,T}(\mathbf{0}) \dot{\bar{W}}_{i,t} \\ &= \frac{1}{T} \sum_{t=1}^T \left(\frac{1}{N} \sum_{i=1}^N \beta_{i,t,0} W_{i,t} \dot{\bar{W}}_{i,t} \right) + \frac{1}{T} \sum_{t=1}^T \left(\frac{1}{N} \sum_{i=1}^N \sum_{s=1}^{t-1} \beta_{i,t,s} W_{i,s} \dot{\bar{W}}_{i,t} \right) + \frac{1}{T} \sum_{t=1}^T \left(\frac{1}{N} \sum_{i=1}^N \varepsilon_{i,t,N,T}(\mathbf{0}) \dot{\bar{W}}_{i,t} \right). \end{aligned}$$

Therefore,

$$\begin{aligned} \frac{1}{N} \sum_{i=1}^N \beta_{i,t,0} W_{i,t} \dot{\bar{W}}_{i,t} &\xrightarrow{p} \dot{\kappa}_{W,\beta,t,t}, \\ \frac{1}{N} \sum_{i=1}^N \sum_{s=1}^{t-1} \beta_{i,t,s} W_{i,s} \dot{\bar{W}}_{i,t} &\xrightarrow{p} \dot{\kappa}_{W,\beta,t,s}, \\ \frac{1}{T} \left(\frac{1}{N} \sum_{i=1}^N \varepsilon_{i,t,N,T}(\mathbf{0}) \dot{\bar{W}}_{i,t} \right) &= \dot{\delta}_t. \end{aligned}$$

A similar argument applies to the denominator and the result follows. \square

B Additional simulation results

		$p(w)$		
		0.25	0.5	0.75
ϕ	0.25	0.044	0.049	0.050
	0.5	0.048	0.050	0.049
	0.75	0.050	0.051	0.057

(a) $\epsilon_{i,t} \sim N(0, 1)$, $N = 1000$

		$p(w)$		
		0.25	0.5	0.75
ϕ	0.25	0.031	0.031	0.034
	0.5	0.048	0.039	0.043
	0.75	0.052	0.047	0.057

(b) $\epsilon_{i,t} \sim \text{Cauchy}$, $N = 50,000$

Table A1: Null rejection rate for the test of the null hypothesis $H_0 : \bar{\tau}_t(1, 0; 0) = 0$ based upon the normal asymptotic approximation to the randomization distribution of $\hat{\tau}_t(1, 0; 0)$. Panel (a) reports the null rejection probabilities in simulations with $\epsilon_{i,t} \sim N(0, 1)$ and $N = 1000$. Panel (b) reports the null rejection probabilities in simulations with $\epsilon_{i,t} \sim \text{Cauchy}$ and $N = 50,000$. Results are computed over 5,000 simulations. See Section 5 of the main text for further details.

		$p(w)$		
		0.25	0.5	0.75
ϕ	0.25	0.044	0.046	0.052
	0.5	0.050	0.054	0.050
	0.75	0.046	0.049	0.054

(a) $\epsilon_{i,t} \sim N(0, 1)$, $T = 1000$

		$p(w)$		
		0.25	0.5	0.75
ϕ	0.25	0.031	0.031	0.034
	0.5	0.048	0.039	0.043
	0.75	0.052	0.047	0.057

(b) $\epsilon_{i,t} \sim \text{Cauchy}$, $T = 50,000$

Table A2: Null rejection rate for the test of the null hypothesis $H_0 : \bar{\tau}_i(1, 0; 0) = 0$ based upon the normal asymptotic approximation to the randomization distribution of $\hat{\tau}_i(1, 0; 0)$. Panel (a) reports the null rejection probabilities in simulations with $\epsilon_{i,t} \sim N(0, 1)$ and $T = 1000$. Panel (b) reports the null rejection probabilities in simulations with $\epsilon_{i,t} \sim \text{Cauchy}$ and $T = 50,000$. Results are computed over 5,000 simulations. See Section 5 of the main text for further details.

		$p(w)$		
		0.25	0.5	0.75
ϕ	0.25	0.050	0.047	0.048
	0.5	0.052	0.052	0.050
	0.75	0.050	0.049	0.048

(a) $\epsilon_{i,t} \sim N(0, 1)$, $N = 100$, $T = 10$

		$p(w)$		
		0.25	0.5	0.75
ϕ	0.25	0.028	0.029	0.032
	0.5	0.046	0.039	0.044
	0.75	0.055	0.044	0.054

(b) $\epsilon_{i,t} \sim \text{Cauchy}$, $N = 500$, $T = 100$

Table A3: Null rejection rate for the test of the null hypothesis $H_0 : \bar{\tau}(1, 0; 0) = 0$ based upon the normal asymptotic approximation to the randomization distribution of $\hat{\tau}(1, 0; 0)$. Panel (a) reports the null rejection probabilities in simulations with $\epsilon_{i,t} \sim N(0, 1)$ and $N = 100$, $T = 10$. Panel (b) reports the null rejection probabilities in simulations with $\epsilon_{i,t} \sim \text{Cauchy}$ and $N = 500$, $T = 100$. Results are computed over 5,000 simulations. See Section 5 of the main text for further details.

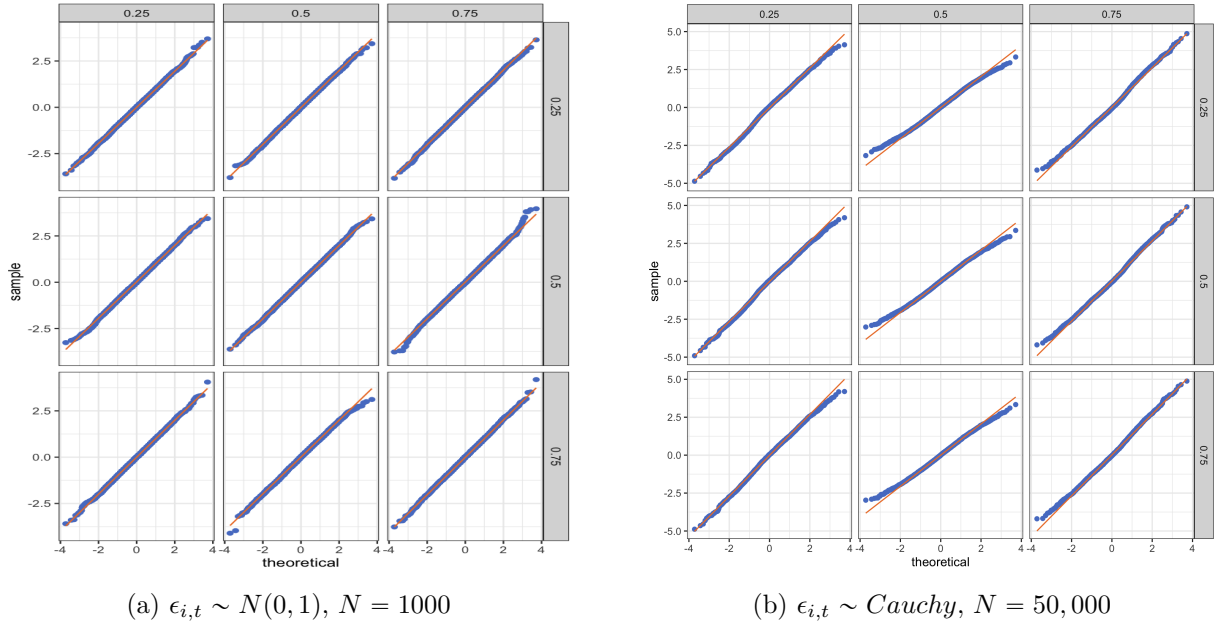


Figure A1: Quantile-quantile plots for the simulated randomization distribution for $\hat{\tau}_t(1, 0; 0)$ under different choices of the parameter ϕ (defined in Example 1) and treatment probability $p(w)$. The quantile-quantile plots compare the quantiles of the simulated randomization distribution (y-axis) against the quantiles of a standard normal random variable (x-axis). The 45 degreee line is plotted in solid orange. The rows index the parameter ϕ , which ranges over values $\{0.25, 0.5, 0.75\}$. The columns index the treatment probability $p(w)$, which ranges over values $\{0.25, 0.5, 0.75\}$. Panel (a) plots the quantile-quantile plots for simulated randomization distribution with normally distributed errors $\epsilon_{i,t} \sim N(0, 1)$ and $N = 1000$. Panel (b) plots the quantile-quantile plots simulated randomization distribution with Cauchy distribution errors $\epsilon_{i,t} \sim \text{Cauchy}$ and $N = 50,000$. Results are computed over 5,000 simulations. See Section 5 of the main text for further details.

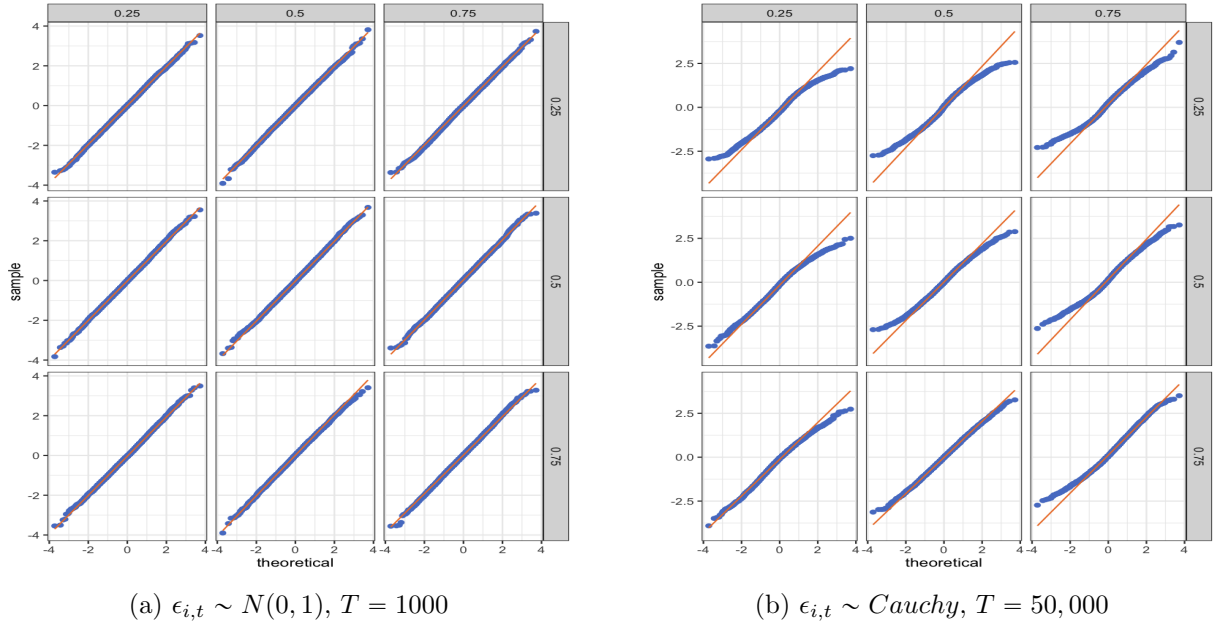


Figure A2: Quantile-quantile plots for the simulated randomization distribution for $\hat{\tau}_i(1, 0; 0)$ under different choices of the parameter ϕ (defined in Example 1) and treatment probability $p(w)$. The quantile-quantile plots compare the quantiles of the simulated randomization distribution (y-axis) against the quantiles of a standard normal random variable (x-axis). The 45 degreee line is plotted in solid orange. The rows index the parameter ϕ , which ranges over values $\{0.25, 0.5, 0.75\}$. The columns index the treatment probability $p(w)$, which ranges over values $\{0.25, 0.5, 0.75\}$. Panel (a) plots the quantile-quantile plots for simulated randomization distribution with normally distributed errors $\epsilon_{i,t} \sim N(0, 1)$ and $T = 1000$. Panel (b) plots the quantile-quantile plots simulated randomization distribution with Cauchy distribution errors $\epsilon_{i,t} \sim \text{Cauchy}$ and $T = 50,000$. Results are computed over 5,000 simulations. See Section 5 of the main text for further details.

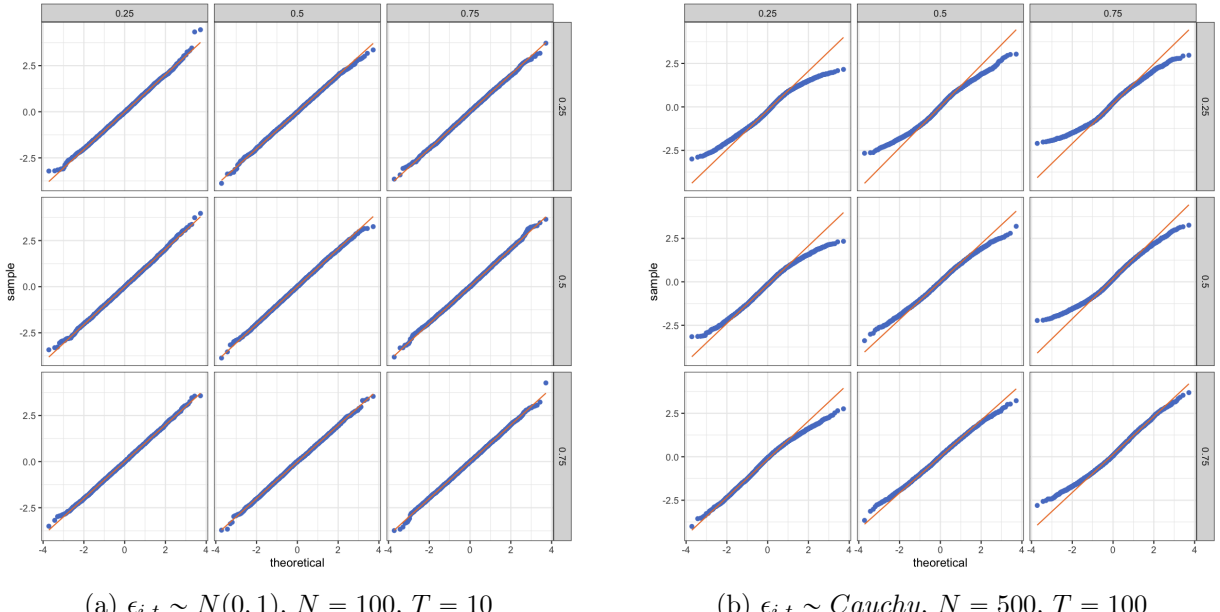


Figure A3: Quantile-quantile plots for the simulated randomization distribution for $\hat{\tau}(1, 0; 0)$ under different choices of the parameter ϕ (defined in Example 1) and treatment probability $p(w)$. The quantile-quantile plots compare the quantiles of the simulated randomization distribution (y-axis) against the quantiles of a standard normal random variable (x-axis). The 45 degreee line is plotted in solid orange. The rows index the parameter ϕ , which ranges over values $\{0.25, 0.5, 0.75\}$. The columns index the treatment probability $p(w)$, which ranges over values $\{0.25, 0.5, 0.75\}$. Panel (a) plots the quantile-quantile plots for simulated randomization distribution with normally distributed errors $\epsilon_{i,t} \sim N(0, 1)$ and $N = 100$, $T = 10$. Panel (b) plots the quantile-quantile plots simulated randomization distribution with Cauchy distribution errors $\epsilon_{i,t} \sim \text{Cauchy}$ and $N = 500$, $T = 100$. Results are computed over 5,000 simulations. See Section 5 of the main text for further details.

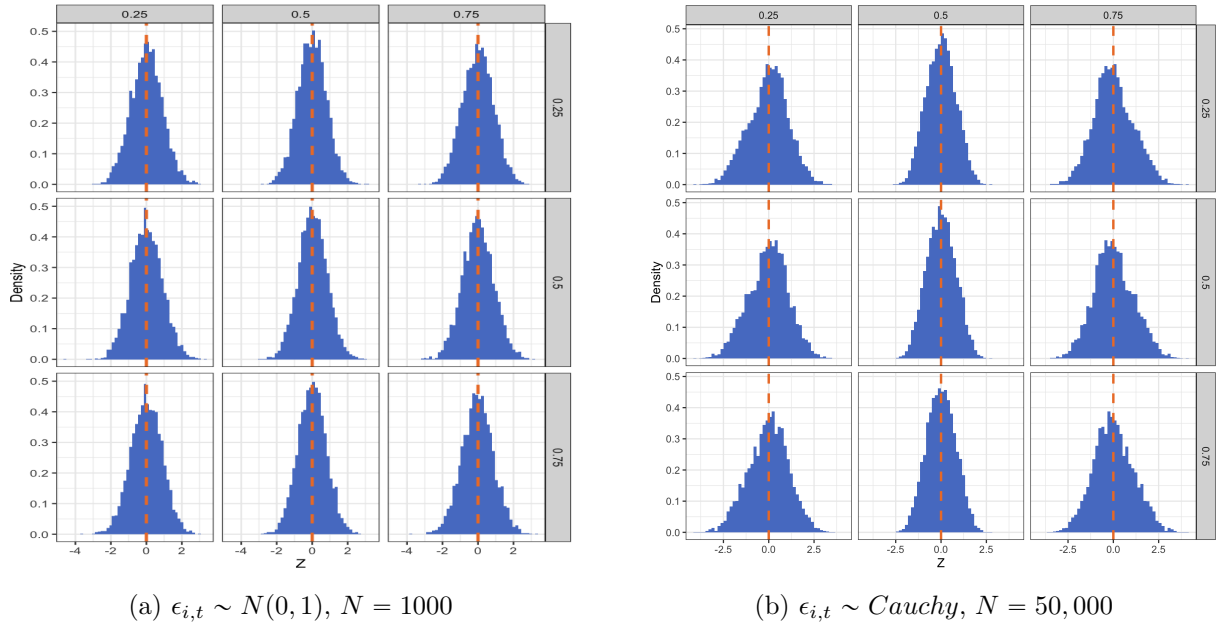


Figure A4: Simulated randomization distribution for $\hat{\tau}_t^\dagger(1,0;1)$ under different choices of the parameter ϕ (defined in Example 1) and treatment probability $p(w)$. The rows index the parameter ϕ , which ranges over values $\{0.25, 0.5, 0.75\}$. The columns index the treatment probability $p(w)$, which ranges over values $\{0.25, 0.5, 0.75\}$. Panel (a) plots the simulated randomization distribution with normally distributed errors $\epsilon_{i,t} \sim N(0, 1)$ and $N = 1000$. Panel (b) plots the simulated randomization distribution with Cauchy distribution errors $\epsilon_{i,t} \sim \text{Cauchy}$ and $N = 50,000$. Results are computed over 5,000 simulations. See Section 5 of the main text for further details.

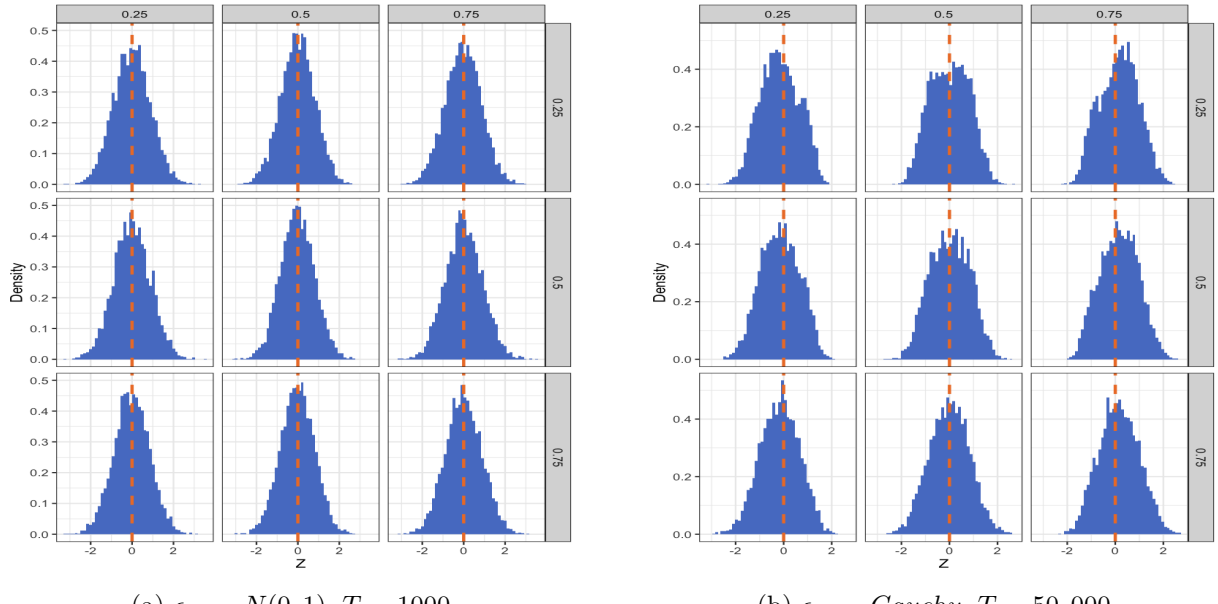


Figure A5: Simulated randomization distribution for $\hat{\tau}_i^\dagger(1,0;1)$ under different choices of the parameter ϕ (defined in Example 1) and treatment probability $p(w)$. The rows index the parameter ϕ , which ranges over values $\{0.25, 0.5, 0.75\}$. The columns index the treatment probability $p(w)$, which ranges over values $\{0.25, 0.5, 0.75\}$. Panel (a) plots the simulated randomization distribution with normally distributed errors $\epsilon_{i,t} \sim N(0, 1)$ and $T = 1000$. Panel (b) plots the simulated randomization distribution with Cauchy distribution errors $\epsilon_{i,t} \sim \text{Cauchy}$ and $T = 50,000$. Results are computed over 5,000 simulations. See Section 5 of the main text for further details.

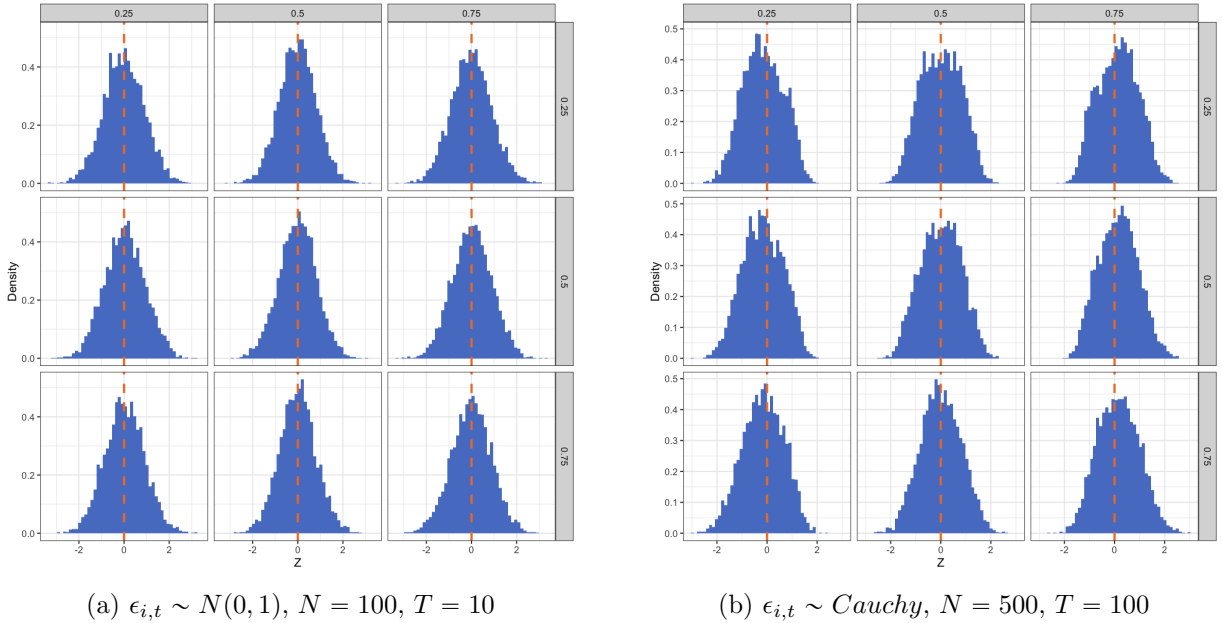


Figure A6: Simulated randomization distribution for $\hat{\tau}^\dagger(1,0;1)$ under different choices of the parameter ϕ (defined in Example 1) and treatment probability $p(w)$. The rows index the parameter ϕ , which ranges over values $\{0.25, 0.5, 0.75\}$. The columns index the treatment probability $p(w)$, which ranges over values $\{0.25, 0.5, 0.75\}$. Panel (a) plots the simulated randomization distribution with normally distributed errors $\epsilon_{i,t} \sim N(0, 1)$ and $N = 100, T = 10$. Panel (b) plots the simulated randomization distribution with Cauchy distribution errors $\epsilon_{i,t} \sim \text{Cauchy}$ and $N = 500, T = 10$. Results are computed over 5,000 simulations. See Section 5 of the main text for further details.

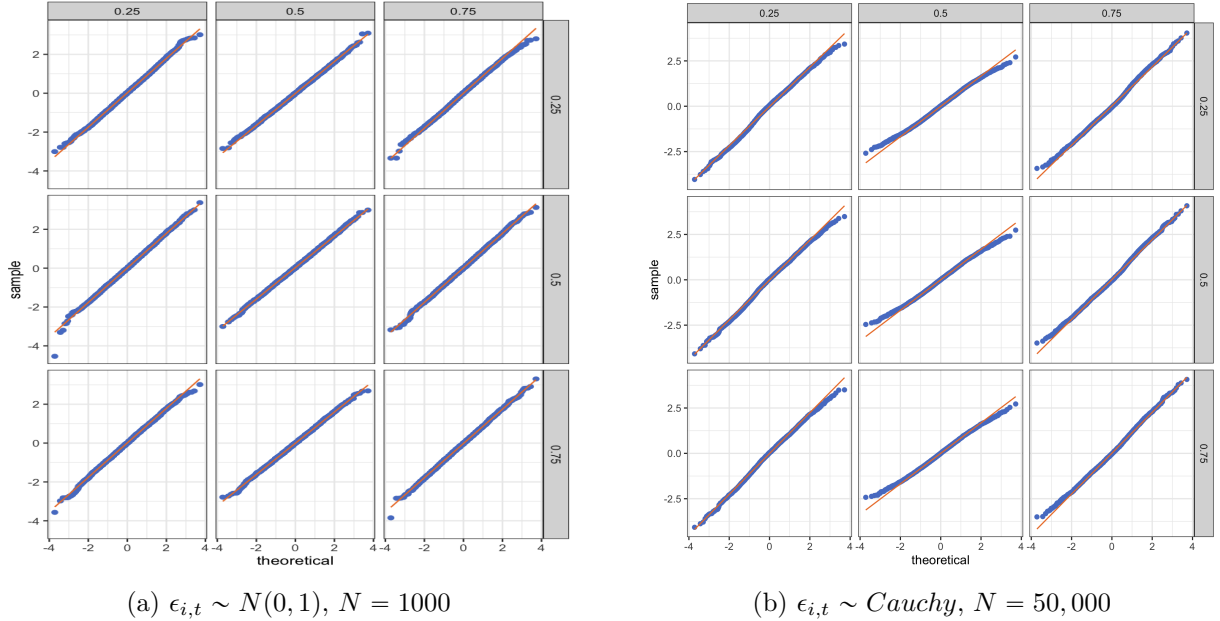


Figure A7: Quantile-quantile plots for the simulated randomization distribution for $\hat{\tau}_t^\dagger(1, 0; 1)$ under different choices of the parameter ϕ (defined in Example 1) and treatment probability $p(w)$. The quantile-quantile plots compare the quantiles of the simulated randomization distribution (y-axis) against the quantiles of a standard normal random variable (x-axis). The 45 degreee line is plotted in solid orange. The rows index the parameter ϕ , which ranges over values $\{0.25, 0.5, 0.75\}$. The columns index the treatment probability $p(w)$, which ranges over values $\{0.25, 0.5, 0.75\}$. Panel (a) plots the quantile-quantile plots for simulated randomization distribution with normally distributed errors $\epsilon_{i,t} \sim N(0, 1)$ and $T = 1000$. Panel (b) plots the quantile-quantile plots simulated randomization distribution with Cauchy distribution errors $\epsilon_{i,t} \sim \text{Cauchy}$ and $T = 50,000$. Results are computed over 5,000 simulations. See Section 5 of the main text for further details.

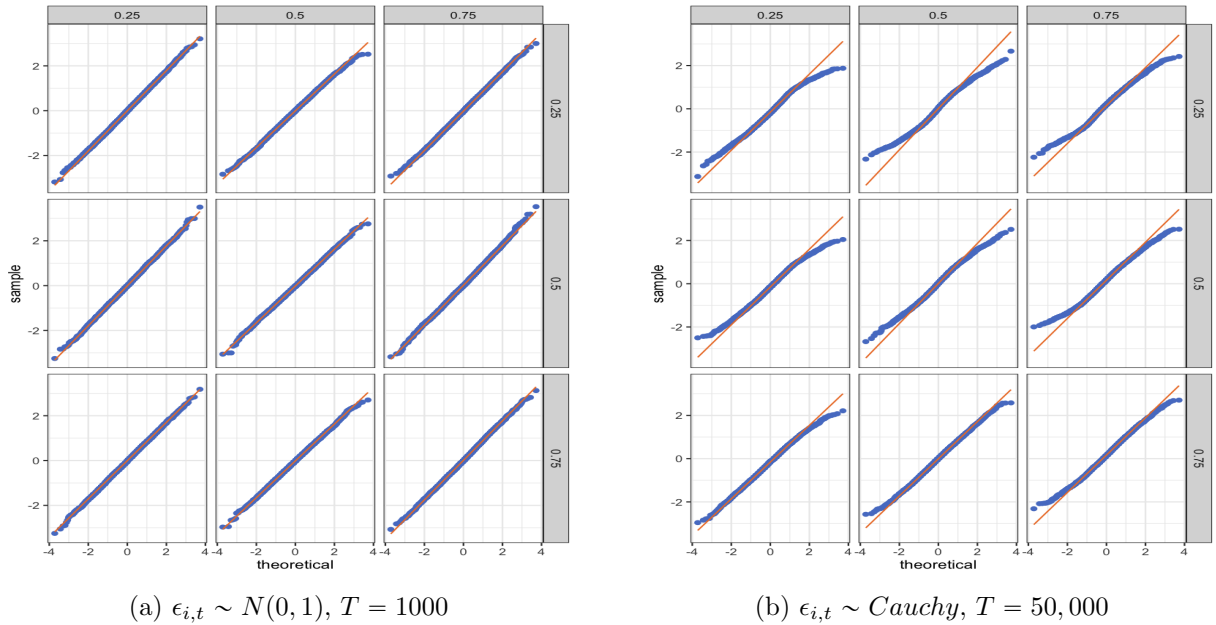


Figure A8: Quantile-quantile plots for the simulated randomization distribution for $\hat{\tau}_i^\dagger(1, 0; 1)$ under different choices of the parameter ϕ (defined in Example 1) and treatment probability $p(w)$. The quantile-quantile plots compare the quantiles of the simulated randomization distribution (y-axis) against the quantiles of a standard normal random variable (x-axis). The 45 degreee line is plotted in solid orange. The rows index the parameter ϕ , which ranges over values $\{0.25, 0.5, 0.75\}$. The columns index the treatment probability $p(w)$, which ranges over values $\{0.25, 0.5, 0.75\}$. Panel (a) plots the quantile-quantile plots for simulated randomization distribution with normally distributed errors $\epsilon_{i,t} \sim N(0, 1)$ and $T = 1000$. Panel (b) plots the quantile-quantile plots simulated randomization distribution with Cauchy distribution errors $\epsilon_{i,t} \sim \text{Cauchy}$ and $T = 50,000$. Results are computed over 5,000 simulations. See Section 5 of the main text for further details.

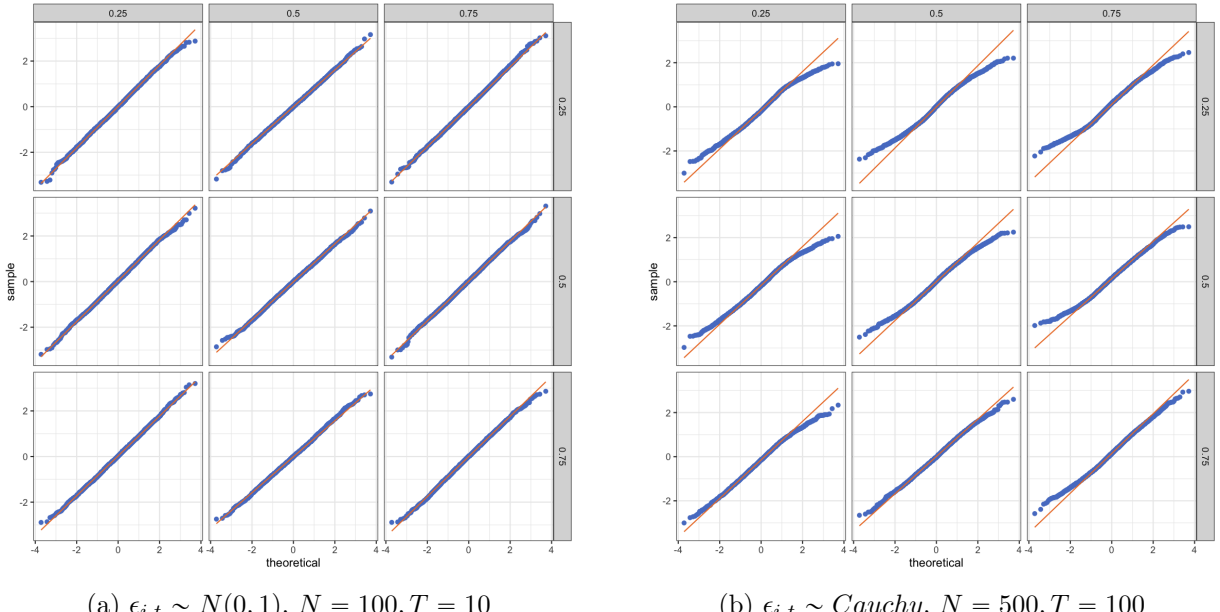


Figure A9: Quantile-quantile plots for the simulated randomization distribution for $\hat{\tau}^\dagger(1, 0; 1)$ under different choices of the parameter ϕ (defined in Example 1) and treatment probability $p(w)$. The quantile-quantile plots compare the quantiles of the simulated randomization distribution (y-axis) against the quantiles of a standard normal random variable (x-axis). The 45 degreee line is plotted in solid orange. The rows index the parameter ϕ , which ranges over values $\{0.25, 0.5, 0.75\}$. The columns index the treatment probability $p(w)$, which ranges over values $\{0.25, 0.5, 0.75\}$. Panel (a) plots the quantile-quantile plots for simulated randomization distribution with normally distributed errors $\epsilon_{i,t} \sim N(0, 1)$ and $T = 1000$. Panel (b) plots the quantile-quantile plots simulated randomization distribution with Cauchy distribution errors $\epsilon_{i,t} \sim \text{Cauchy}$ and $T = 50,000$. Results are computed over 5,000 simulations. See Section 5 of the main text for further details.

C Additional empirical results

As in Section 6, we begin by estimating unit-specific, weighted average dynamic causal effects to investigate the causal effect of $W = 1\{\lambda \geq 0.6\}$ on the total payoffs earned. We focus on the same two units as in Figure 7, Figure A10 plots the nonparametric estimates $\hat{\tau}_{i,t}(1, 0; 0)$ for $t \in [T]$ for the total payoffs outcome.

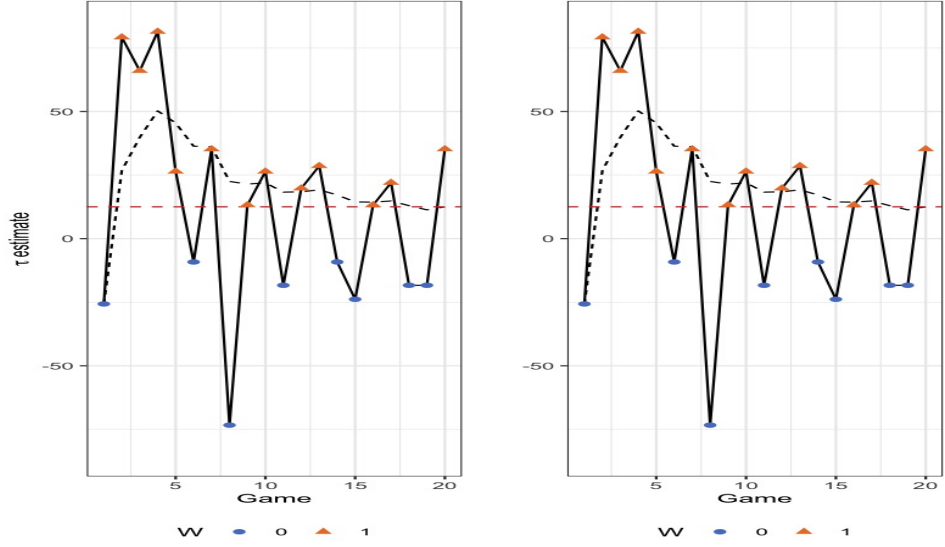


Figure A10: Estimates of the weighted average i, t -th lag-0 dynamic causal effect (Definition 6) of $W = 1\{\lambda \geq 0.6\}$ on total stage game payoffs for two units in the experiment of [Andreoni and Samuelson \(2006\)](#). The solid black line plots the nonparametric estimator $\hat{\tau}_{i,t}(1, 0; 0)$. The dashed black line plots the running average of the period-specific estimator for each unit; that is, for each $t \in [T]$, $\frac{1}{t} \sum_{s=1}^t \hat{\tau}_{i,s}(1, 0; 0)$. The dashed red line plots the estimated unit- i lag-0 average weighted dynamic causal effect, $\hat{\tau}_i(1, 0; 0) = \frac{1}{T} \sum_{t=1}^T \hat{\tau}_{i,t}(1, 0; 0)$.

We next estimate period-specific, weighted average dynamic causal effects for each time period $t \in [T]$ and $p = 0, 1, 2, 3$. The results are plotted in Figure A11. It also plots the nonparametric estimator the total lag- p weighted average causal effect $\hat{\tau}^\dagger(1, 0; p)$ for $p = 0, 1, 2, 3$. While of course the units are different, the qualitative results are unchanged from Section 6. We find strong evidence of a contemporaneous causal effect on the total payoffs but mixed evidence on dynamic causal effects.

Finally, Figure A12 plots the randomization distributions under the sharp null of no dynamic causal effects for $p = 0, 1, 2, 3$ along with the point estimate $\hat{\tau}^\dagger(1, 0; p)$ at the realized treatment panel. As before, the randomization distributions appear to be smooth and symmetric around zero. We reject the sharp null of no dynamic causal effects at the 5% level for $p = 0$ (p-value is 0.0071) but are unable to do so for $p = 1, 2, 3$.

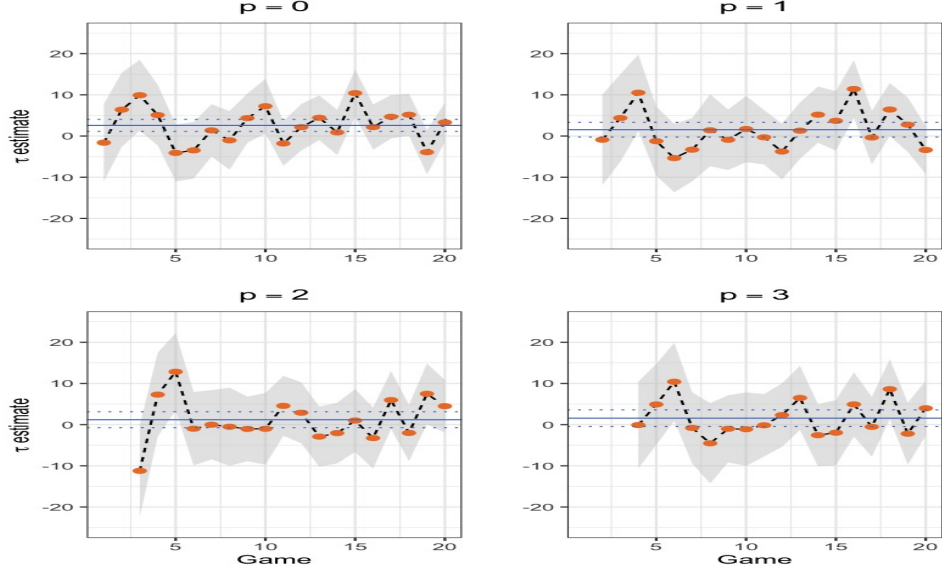


Figure A11: Estimates of the time- t lag- p weighted average dynamic causal effect, $\tau_t^\dagger(1,0;p)$ of $W = 1\{\lambda \geq 0.6\}$ on total payoffs based on the experiment of [Andreoni and Samuelson \(2006\)](#) for each time period $t \in [T]$ and $p = 0, 1, 2, 3$. The black dashed line plots the nonparametric estimator of the time- t lag- p weighted average dynamic causal effect, $\hat{\tau}_t^\dagger(1,0;p)$, for each period $t \in [T]$. The grey region plots the 95% point-wise confidence interval for $\tau_t^\dagger(1,0;p)$ based on the conservative estimator of the asymptotic variance of the nonparametric estimator (Theorem 3.2). The solid blue line plots the nonparametric estimator of the total lag- p weighted average dynamic causal effect, $\hat{\tau}^\dagger(1,0;p)$ and the dashed blue lines plot the 95% confidence interval for $\tau^\dagger(1,0;p)$ based on the conservative estimator of the asymptotic variance of the nonparametric estimator.

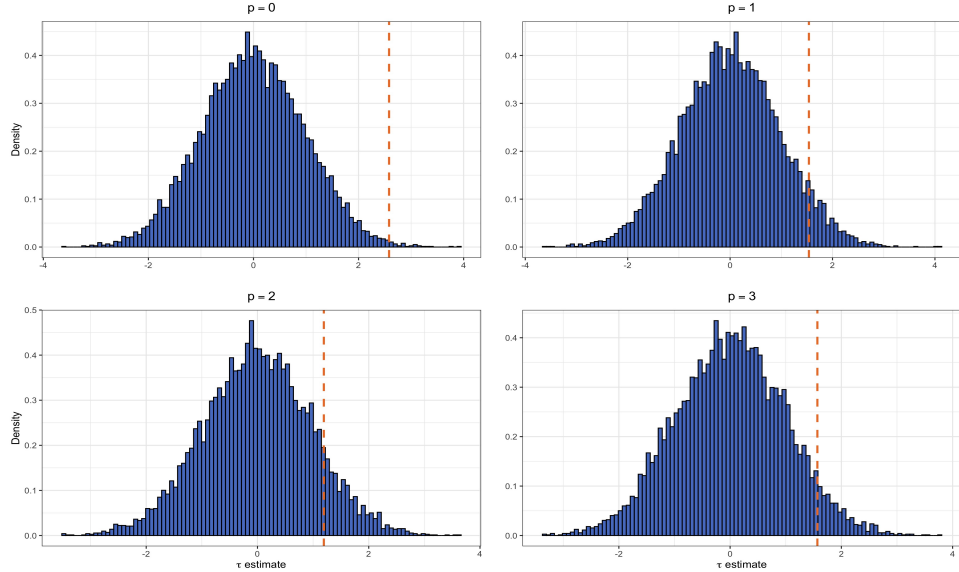


Figure A12: Estimated randomization distribution of the nonparametric estimator of the total lag- p weighted average dynamic causal effect, $\hat{\tau}^\dagger(1,0;p)$, under the sharp null of no dynamic causal effect, $\tau_{i,t}(w,w;p) = 0$ for all $i \in [N], t \in [T]$. The dashed orange line plots the estimate, $\hat{\tau}^\dagger(1,0;p)$ at the realized treatments in the experiment of [Andreoni and Samuelson \(2006\)](#). The estimated randomization distributions are constructed based on 10,000 draws.

	lag- p			
	0	1	2	3
Point estimate, $\hat{\tau}^\dagger(1, 0; p)$	2.580	1.538	1.192	1.568
Conservative p-value	0.000	0.092	0.226	0.127
Randomization p-value	0.007	0.116	0.213	0.107

Table A4: Estimates of the total lag- p weighted average dynamic causal effect for $p = 0, 1, 2, 3$. The conservative p-value reports the p-value associated with testing the weak null hypothesis of no average dynamic causal effects, $H_0 : \tau^\dagger(1, 0; 0) = 0$, using the conservative estimator of the asymptotic variance of the nonparametric estimator (Theorem 3.2). The randomization p-value reports the p-value associated with randomization test of the sharp null of dynamic causal effects, $H_0 : \tau_{i,t}(w, \tilde{w}; 0) = 0$ for all $i \in [N], t \in [T]$. The randomization p-values are constructed based on 10,000 draws.